

## **General Disclaimer**

### **One or more of the Following Statements may affect this Document**

- This document has been reproduced from the best copy furnished by the organizational source. It is being released in the interest of making available as much information as possible.
- This document may contain data, which exceeds the sheet parameters. It was furnished in this condition by the organizational source and is the best copy available.
- This document may contain tone-on-tone or color graphs, charts and/or pictures, which have been reproduced in black and white.
- This document is paginated as submitted by the original source.
- Portions of this document are not fully legible due to the historical nature of some of the material. However, it is the best reproduction available from the original submission.

Contract No. NAS 9-14707

Line Item No. 3

DRD No. MA-183TA

DRL No. T-1057

# **BALLISTIC SIGNATURE IDENTIFICATION SYSTEMS STUDY**

**14 May 1976**

(NASA-CR-147798) BALLISTIC SIGNATURE  
IDENTIFICATION SYSTEMS STUDY Final Report  
(Grumman Aerospace Corp.) 48 p HC \$4.00

N76-27249

CSCL 14B

Unclas

G3/09 44551

**GRUMMAN**

Contract No. NAS 9-14707

Line Item No. 3

DRD No. MA-183TA

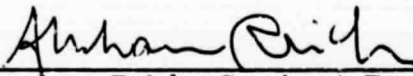
DRL No. T-1057

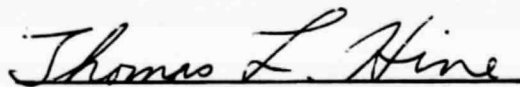
BALLISTIC SIGNATURE IDENTIFICATION

SYSTEMS STUDY

14 May 1976

Prepared by:

  
Abraham Reich, Cognizant Engineer

  
Thomas L. Hine, Section Head

Grumman Aerospace Corporation  
Bethpage, New York 11714

## Table of Contents

<u>Title</u>	<u>Page</u>
ABSTRACT . . . . .	iv
INTRODUCTION . . . . .	1
TECHNICAL INVESTIGATIONS . . . . .	2
Cone Manufacture and Bullet Mount . . . . .	2
Illumination of the Bullet . . . . .	2
Coherent Optical Processor . . . . .	3
Holographic Lens Matrix Evaluation . . . . .	6
Tilt Tests . . . . .	6
Model Bullet Simulation . . . . .	8
Unitech Photography . . . . .	8
Photopolymer Study . . . . .	8
FUTURE WORK . . . . .	9

PRECEDING PAGE BLANK NOT FILMED

PRECEDING PAGE BLANK NOT FILMED



## ABSTRACT

This final report of a Ballistic Signature Identification System Study performed under NASA Contract NAS 9-14707 describes the results of an attempt to establish a uniform procedure for documenting (recording) expended bullet signatures as effortlessly as possible and to build a comprehensive library of these signatures in a form that will permit the automated comparison of a new suspect bullet with the pre-stored library. The ultimate objective is to achieve a standardized format that will permit nationwide interaction between police departments, crime laboratories, and other interested law enforcement agencies.

## INTRODUCTION

This final report covers a Ballistic Signature Identification System Study done under NASA Contract NAS 9-14707. The period of work was August 1975 to March 1976.

The ultimate objective is to establish a uniform procedure for documenting (recording) expended bullet signatures as effortlessly as possible and to build a comprehensive library of these signatures in a form that will permit the automated comparison of a new suspect bullet with the prestored library. If this process can be accomplished in a standardized format, it will permit nationwide interaction between police departments, crime laboratories, and other interested law enforcement agencies.

The initial effort covered under this program had a twofold purpose. The first was to explore bullet signature recording techniques to isolate those techniques most likely to be successful in an automated system. The second purpose was to process (identify) the signatures in a Grumman Coherent Optical Processor, to determine the potential feasibility of automated bullet identification.

A variety of signature recording configurations were tried, including:

- A static reflecting cone for  $2\pi$  rad ( $360^\circ$ ) signature documentation. This technique was explored in a variety of setups.
- A  $\pi$  rad ( $180^\circ$ ) side view configuration. This configuration was used to estimate the performance to be expected from a rotating bullet exposed to a slit camera.
- A photopolymer dip recording technique.

The conclusions reached during this effort are essentially that the first and third procedures listed deserve further work - under improved conditions. The stainless steel recording cone was of limited performance capability. A pyrex glass reflecting cone is expected to give much improved performance. Since this static technique does record the entire signature in one simple exposure, it has outstanding latent merit, and should be explored more fully.

The photopolymer dip technique, as described herein, provides a completely different method of recording the bullet signature. It can be simple and fast. However, it was discovered only late in the program and does deserve further effort.

The bullet identification procedures explored with the Coherent Optical Processor lead us to conclude that, at best, the automated procedure could appreciably narrow the suspect library search procedure. The ultimate decision would be made manually, working with a much smaller file of possible matches. However, the considerable reduction in search time could bring national cooperation between law enforcement people closer to reality.

## TECHNICAL INVESTIGATIONS

### CONE MANUFACTURE AND BULLET MOUNT

One piece of equipment developed for this program was the cone used to photograph the spent rounds. This cone, with a highly reflective surface angle at  $\pi/4$  rad ( $45^\circ$ ), ensured that the entire 360-degree surface of the round could be photographed in one exposure without special cameras or time-consuming photographic techniques.

The cone was manufactured inhouse at Grumman Aerospace Corporation (GAC) for two reasons. One, was the time element involved (one week versus eight or more weeks if done out-of-house) and the other was the cost savings (\$600 versus \$2000, or more).

Stainless steel was selected for the cone because of its ability to polish well and to withstand nicks and corrosion. The cone was machined on a lathe from a 0.127m (five-inch) square by 0.04m (1-5/8 inch) thick block of high temperature stainless steel. The opening at the top of the cone measured 0.102m (four inches) in diameter while the opening at the base of the cone measured  $1.81 \times 10^{-2}$ m (0.75 inch).

A major problem with the cone material was the randomly spaced defects (pits) inherent in the metal volume that kept appearing at different parts of the cone regardless of the amount of polishing. Because of this, a high quality homogeneous reflective surface could never be achieved. Improved reflecting cones should be made from glass in the future, and coated so that the irregularities experienced with the metal surface are eliminated. Figure 1 is a photograph of the cone.

The requirement to hold the bullet so that it could be inserted into the cone and be adjusted for optimum focus resulted in the assembly depicted in Figure 2. The holding fixture is a Jacobs chuck mounted to a  $5.08 \times 10^{-2}$ m square (2 x 2 inch) metal plate. The plate/chuck arrangement is inserted into a GAC manufactured (matched filter) holder. The filter holder has adjustable X and Y axis controls (Figure 3). By proper adjustment of the X and Y controls, maximum resolution of the bullet's characteristics can be achieved. Inserted into the chuck is a circular rod with a machined end. Beeswax attached to this end supplies the adhesive force necessary to hold the bullet.

### ILLUMINATION OF THE BULLET

Several lighting techniques were evaluated to obtain maximum brightness, contrast, and resolution. These included coherent and noncoherent rear illumination, as well as coherent and noncoherent front illumination as described here:

- Coherent rear illumination: For evaluating rear illumination with a coherent light source (a helium-neon 5 milliwatt laser), the bullet was placed on a clear glass plate with double-backed tape. The bullet was centered at the bottom of the cone and the glass plate was then fixed to the base of the cone. Laser light was then directed through the glass illuminating the bullet surface; the latter could be seen by reflection from the cone surface. Figure 4 is a photograph of this technique. Note the d.c. block used to prevent on-axis rays from entering the camera lens. This method was proved not practicable because of laser speckling, which reduced the resolving capabilities of the arrangement.

Speckling is a condition that is usually associated with coherent laser light. Coherence implies that all the light waves emitted by the laser are in phase with each another. If waves originating from a point meet at a point and are still in phase they will reinforce each another and a bright point is evident. Should they meet out of phase at a point, they will cancel and diminished light, to no light, is seen at this point. A perfectly smooth surface such as glass or a mirror will cause the waves to stay in phase, resulting in even illumination. Should there be slight irregularities in the surface (and here we are considering fractional wavelengths of light) then there will result random light and dark areas, or speckling. Because of the inability to develop a mirror-like finish on the cone surface, the speckling produced was instrumental in eliminating this method of illumination.

- Noncoherent rear illumination: The laser was replaced with a noncoherent light source, consisting of a microscope lamp and focusing optics. A slight improvement in resolution was noted but the system suffered from uneven illumination or "hot spots" on certain areas of the cone surface. This condition is illustrated in Figure 5
- Front illumination with beamsplitter: The next approach assessed was to illuminate the cone from the front using a beamsplitter and microscope lamp (Figure 6). Although this method improved the brightness and resolution over the previous methods, it had the major disadvantage of producing "ghost" images. These images were caused by secondary reflections from the beamsplitter, as illustrated in Figure 7. The ghost images can be seen in Figure 8.
- Front Illumination Using circular fluorescent lamp: Two changes were made for further evaluation of the lighting techniques; one was to change the magnification of the camera to obtain more pertinent bullet information on the 35 mm frame; the second was to illuminate the bullet with a circular fluorescent bulb.

The camera magnification was increased by adding a 2X tele-extender and replacing the existing 50 mm F/2.0 NIKON lens with an F/3.5 Micro-Nikkor lens. The camera was mounted so that it was in the center of the lamp and coaxial with the cone. Figure 9 illustrates this set-up. This technique improved the photography by providing even illumination of the cone and in producing a magnified image that resulted in more detail being recorded. Improvements in the size and shape of the d.c. stop were also made at this time.

## COHERENT OPTICAL PROCESSOR

Before discussing the details of the tests run with the GAC Coherent Optical Processor, a brief description of the system and some of its components is given. Figure 10 shows the layout of the signal processor. The raw laser beam, which is quite narrow upon emission (~1mm), is reflected and redirected by two corner mirrors. A beamsplitter divides the beam into two equal half-power beams. Spatial filters pass the raw laser beams and remove all unwanted optical noise and harmonics and produce diverging, uniform, noise-free beams. The collimating lenses convert the diverging spherical beams into collimated plane waves. Both the signal beam and the reference beam are processed in this manner. The bullet imagery containing the signature produced in firing, is inserted in the film transport and modulates the signal beam. The bullet-modulated beam is then incident on the holographic lens matrix. This holographic lens matrix, a GAC developed device,



can perform the functions of many lenses although it is physically only a single glass plate. As many as 100 lenses, in 10 X 10 two-dimensional format, have been manufactured and used. Figure 11 is a photograph of a 10 X 10 matrix. When the laser beam traverses the holographic lens Fourier Transforms are imposed on the bullet imagery inserted into the beam. The Fourier transform is exhibited in the diffraction pattern formed. Figure 12 is a magnified diffraction pattern of bullet B-10. This pattern, which is extremely small ( $\sim 50 \mu$  radius) and is unique to that bullet, is recorded and stored on a photographic glass plate as a matched filter.

The matched filter is made by recording both amplitude (the diffraction pattern) and phase relationships of the image. This is accomplished by exposing the photographic recording plate to the reference beam (a collimated plane wave) at the focal positions of the holographic lenses while recording the diffraction pattern. This results in the diffraction pattern having a grating structure superimposed on it. Figure 13 shows how the diffraction pattern of a square becomes a matched filter. By adjusting the intensity of either the signal beam or the reference beam through neutral density filters (attenuators), the grating can be shifted from the low frequency (near d.c.) range of the spectrum to the high frequency portion of the spectrum, or anywhere in between. The setting of the passband is determined by the recognition requirements. Gross object shapes can be obtained by highlighting the d.c.-to-low frequency part of the spectrum, whereas the high frequency portions of the spectrum contain the fine details of a scene.

Identification of an unknown suspect object is obtained with this technique when the diffraction pattern of the unknown is "matched" with a diffraction pattern previously stored on film as a matched filter. The matched filter (Figure 14), having been prepared essentially as a hologram, will generate from all areas of the diffraction pattern that precisely overlap and contain the correct conjugate phase collimated reference beam (Figure 15). A lens located behind the filter gathers the collimated light and focuses it onto a photodetector or closed circuit television system.

Several versions of bullet imagery photographs were tested during this program. They were (a) bullets photographed in the reflecting cone, (b) front view of the bullet with edge lighting, (c) magnified portions of the bullet, and (d) a synthesized model of a bullet mounted in a cone. In all but the last case a reference bullet was put into the matched filter memory bank and measurements were taken to evaluate how other bullets from the reference gun and other guns played back. (The last case will be discussed separately.)

The first signature recording configuration tried was to illuminate the bullet in the reflecting cone from the front, using a pellicle beamsplitter (to remove ghost images) and a microscope lamp. A matched filter made from this configuration showed strong playback for the reference bullet itself, but weak outputs for the other bullets fired from the same gun. Similar results were obtained when certain portions of the imagery, that were primarily non-signature in character, were painted out. Again, the reference bullet output was significantly higher (1900 millivolts) than that of other similar bullets (300 millivolts). These results indicated that not enough information relating to the bullet's firing signature were being recorded.

It was then decided to try, as input imagery, photographs showing one side of the bullet (Figure 16). A matched filter was made of bullet A-3. Identification runs showed that bullet A-3 autocorrelated with bullets A-1, A-2, and A-4 from the same weapon. Analysis of the diffraction pattern showed that knurling on the bullet was the major feature

contributing to the diffraction pattern. Another run was made with the knurling painted out. A slight improvement was noted in that two of the four bullets from the same weapon played back correctly, and none of the bullets from the other guns did.

Based on this finding, bullet B-10 was edge-lighted and a mirror placed on the back side as a reflector. The bullet was registered through finding a land that had a characteristic bend unique to that bullet and other bullets from that gun. Figure 17 shows the registration mark used. Photographs of these bullets were made and B-10 was used as the reference bullet. Another adjustment made at this time was to mask down the 70 mm window of the available film transport so that noncontributing laser light was eliminated. The shape of the aperture approximated a bullet shape. The matched filter was optimized to record the 4 to 8 ring area of the diffraction pattern. With B-10 in memory as a reference, encouraging results were obtained for the first time. Table 1 lists the bullets and their respective outputs.

TABLE 1 BULLETS AND RESPECTIVE OUTPUTS

<u>BULLET</u>	<u>OUTPUT, MILLIVOLTS</u>
B-10	1700
B-9	1100
B-8	1100
B-7	700
A-8	700
A-7	1000
A-6	500
A-5	600

Figures 18 through 25 show the respective output signals.

With the results achieved above, the next step was to double the number of bullets on the film strip to sixteen. Several attempts were made at duplicating the results of the successful run of eight bullets with the sixteen-bullet imagery, but none were as successful. B-10 was again chosen as the reference bullet and care was taken to maintain the conditions that existed for the eight-bullet run (i.e., exposure, lighting, registration, etc.). On playback with the new film input not all the B series bullets were recognized and some of the A, C, and D series bullets did play back. Magnified views of both B-10 reference bullets show that the second bullet lacks signature detail and has a washed out appearance compared to the successful B-10. This is attributed to the particular edge-lighting angle used in the sixteen-exposure run. This angle is set subjectively, depending on how the operator views the scene.

A series of tests were run of previously exposed film that had been magnified with A Durst enlarger. This approach proved unsuccessful due to inconsistent lighting across the bullet area of interest, resulting in uneven distribution of signature from bullet to bullet. Figures 26 and 27 are examples of this inconsistency.

## HOLOGRAPHIC LENS MATRIX EVALUATION

Another factor investigated was to insure that the holographic lens matrix was capable of properly resolving the high-frequency signature content of the bullets. To verify this, the holographic lens was replaced with a high quality Schneider 360mm lens. The film strip of eight bullets was inserted into the film transport and B-10 again was chosen as the reference bullet. Again, good results were obtained with the film strip. Table 2 lists the output signals achieved.

TABLE 2 OUTPUT SIGNALS ACHIEVED

<u>BULLET</u>	<u>OUTPUT, MILLIVOLTS</u>
B-10	600
B-9	300
B-8	350
B-7	325
A-8	100
A-7	250
A-6	275
A-5	275

This test was repeated for the sixteen-bullet film strip using B-10 again as reference. Table 3 shows the unsuccessful results.

These tests verified that the holographic lens matrix in the Processor has sufficient resolution capability to process high-frequency information of bullets. This test also verified that there are some meaningful differences in the two film strips that enable one strip to properly identify the bullets while the other cannot. Magnified photos of all the bullets (and calibrating them against the reference bullets) show some slight tilt and rotational differences, but nothing outstanding. The bullet diameters were also measured to ensure that no meaningful scale changes were introduced. Micrometer measurements show a variation of only  $1.27 \times 10^{-4}$  m (0.005 inch) between rounds.

### TILT TESTS

The following test was devised to determine the effect a tilted bullet would have on the recognition output signal: Take a series of photographs of a bullet as it is tilted from 0 to 10°, in one-degree increments. Put the 0-degree bullet in memory and compare the recognition output signal it produces with that of the tilted bullets.



TABLE 3 UNSUCCESSFUL RESULTS

<u>BULLET</u>	<u>OUTPUT, MILLIVOLTS</u>
B-10	350
B-9	100
B-8	100
B-7	175
A-8	225
A-7	275
A-6	200
A-5	175
C-8	200
C-7	-
C-6	200
C-5	200
D-8	100
D-7	250
D-6	175
D-5	150

Table 4 shows the results of the test:

TABLE 4 TEST RESULTS

<u>ROTATION, DEGREES</u>	<u>OUTPUT, MILLIVOLTS</u>
0	2000
1	2000
2	1750
3	1750
4	1250
5	1250
6	1000
7	750
8	500
9	400
10	-

These results coincide closely with results seen in other laboratory tests previously conducted with other types of inputs. A six-degree excursion will result in a decrease to one-half of the signal output.

Based on the results produced by the various tests, it was decided to utilize the remaining time primarily on the reflecting recording device.

#### MODEL BULLET SIMULATION

To determine just how sensitive the Processor is to changes in land and groove configuration of a bullet mounted in the reflecting cone, and to ascertain the optical bandpass filter required, a model bullet was synthesized. A two-dimensional scaled replication of a bullet mounted in a cone was drawn on vellum paper with India ink. The lands and grooves were spaced to represent a typical fired round. A ratio of 0.74 between the inner ring diameter and the outer ring diameter was used as representative of the situation when a real bullet is mounted in the cone.

A series of photographs was taken during which the lands and grooves were eliminated one at a time, until only the annulus was left. Two other photographs were taken of randomly spaced lands and grooves to simulate different bullets, to produce cross-correlation outputs. A series of filters containing different passbands was made of the first "bullet" and the other "bullets" played back through it. The voltage outputs versus land and groove configuration are illustrated in figures 28, 29, and 30. Matched filters corresponding to each plot are shown in figures 31 through 36. As the filter bandpass becomes increasingly higher, the signal-to-noise ratio and the sensitivity of the filter decreases. This is especially true for the very high pass filter. Initial results indicate that the filter should be optimized at a linear radius of  $18.6 \times 10^{-4}$  cm ( $7.3 \times 10^{-4}$  in.) and  $29.5 \times 10^{-4}$  cm ( $1.16 \times 10^{-3}$  in.) for the optics and laser wavelength currently being used.

#### UNITECH PHOTOGRAPHY

A series of photographs was taken of bullets fired by New York City Police Department and supplied to Unitech, Inc. of Austin, Texas. These photographs were made using 35 mm Kodak Panatomic-X film, a panchromatic film that yields negatives with extremely fine grain and excellent definition. It has an ASA rating of 32. The photographs were taken with a Nikon-F 35 mm camera using an F/3.5 Micro-Nikkor lens and a Spiratone 2X tele-extender. Exposures were made at F/22 for 20 seconds with illumination supplied by a 22 watt circular fluorescent lamp. All bullets were cone mounted. The film was then processed in Microdal-X developer for eight minutes at  $21.1^{\circ}\text{C}$  ( $70^{\circ}\text{F}$ ).

#### PHOTOPOLYMER STUDY

As a side study during the program, an attempt was made to determine if photopolymer film could be used to provide bullet signature imagery for the Processor. This photopolymer, manufactured by duPont, consists of an acrylate-type photopolymerizable monomer, an initiator, a cellulose polymer binder, and a dye sensitizer. It can be coated on glass plates to thicknesses of 50 to 150 microns.

The material is designed for holographic work. After exposing to light, the material is totally polymerized and the dye bleached with uniform fluorescent light. The material can be potted, if desired, between glass plates using optical grade epoxy. Once potted, the material lasts indefinitely and is impervious to dust and scratches. It becomes a permanent optical device.

With this in mind, bullet dipping and rolling procedures were initiated whereby the bullet was dipped or rolled in photopolymer to see if a "footprint" of the bullet's surface characteristics could be faithfully recorded. It was quickly realized that rolling the bullet in photopolymer coated on a glass substrate was not very effective. Dipping, however, was much more successful. Earlier dipped bullets exhibited bubbles of trapped air, from repeated dippings. By thinning the photopolymer with methyl chloride and using only two dips, a coating free of bubbles was achieved. By allowing the bullet to dry in a closed but not airtight compartment, uniform drying was achieved resulting in a coating that, after removal with tweezers, was found to have recorded almost all of the bullet's surface characteristics. Figure 37 is an enlarged view of the recording. After removal, the strip is sandwiched between two glass plates and exposed to the UV of the fluorescent lamp. The coating changes from a reddish-orange to an almost transparent yellow.

A Schlieren system (see Figure 38 and Appendix A) has been set up to enhance the recording so that more definitive signature information may be realized.

#### FUTURE WORK

Follow-on work to this first effort would include obtaining more data from the bullet model regarding focusing, rotation, contrast ratio, etc. and applying these data to more detailed tests of cone imagery. The present cone should be replaced by one made of pyrex glass and coated so that higher resolution and reflectivity will be available.

Work with the photopolymer dip technique should be continued with emphasis on obtaining, evaluating, and processing recorded photopolymer strips.

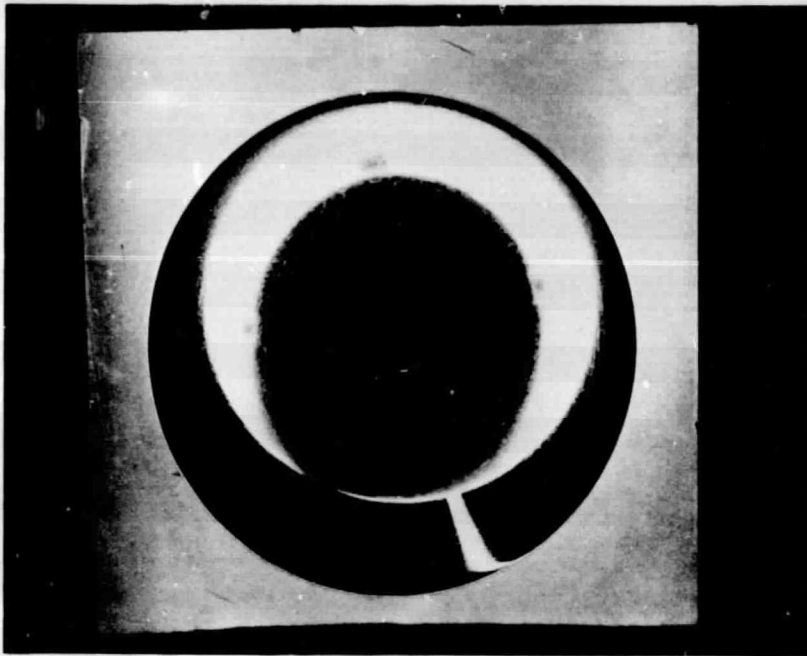


**Fig. 1 Photo of 45° Cone**

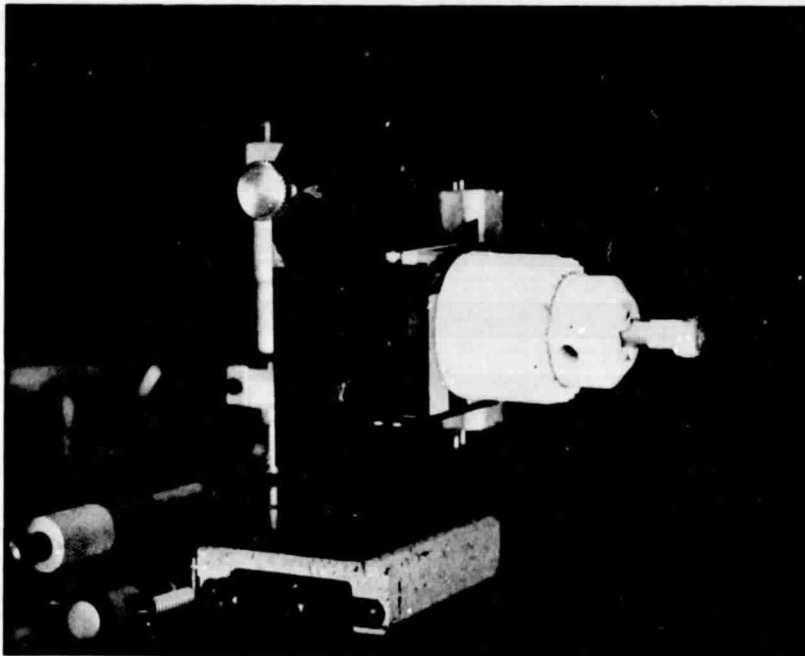


**Fig. 2 Chuck Assembly and Positioner. Chuck is Mounted to GAC Matched Filter Assembly**

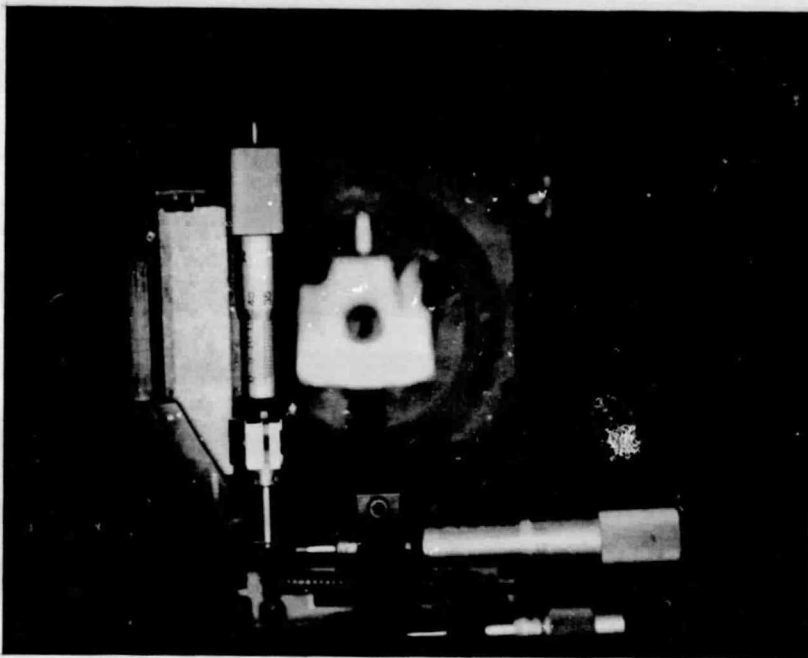


**Fig. 3 X & Y Axis Positioning Controls for Centering the Bullet**

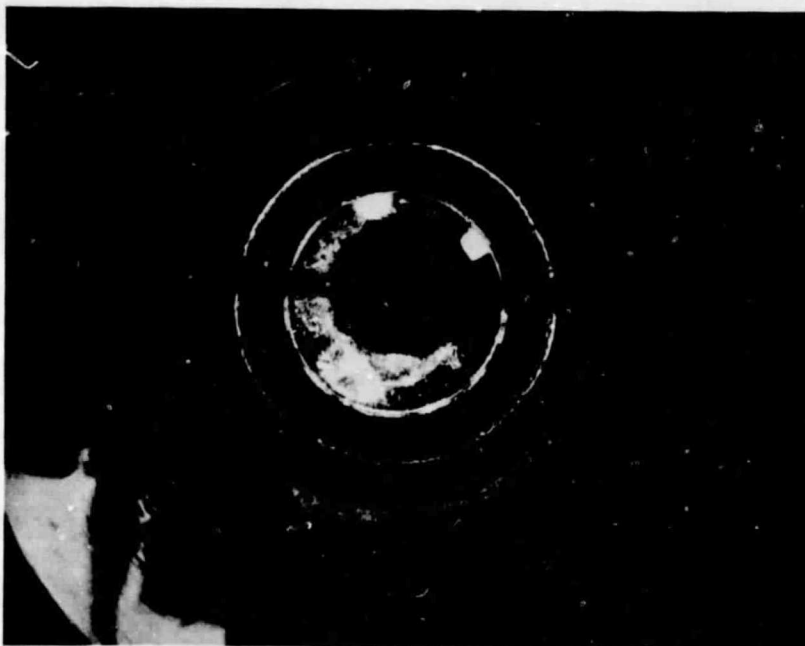


**Fig. 4 Speckling Due to Rear Illumination with Laser Beam**

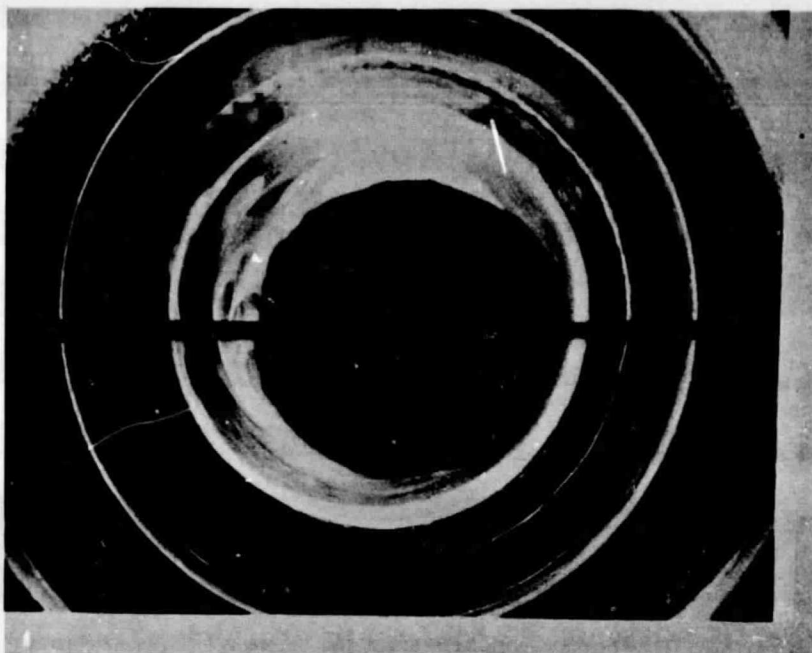


**Fig. 5 Hot Spots Formed by Rear Illumination With Noncoherent Light Source. Note Large D.C. Block.**

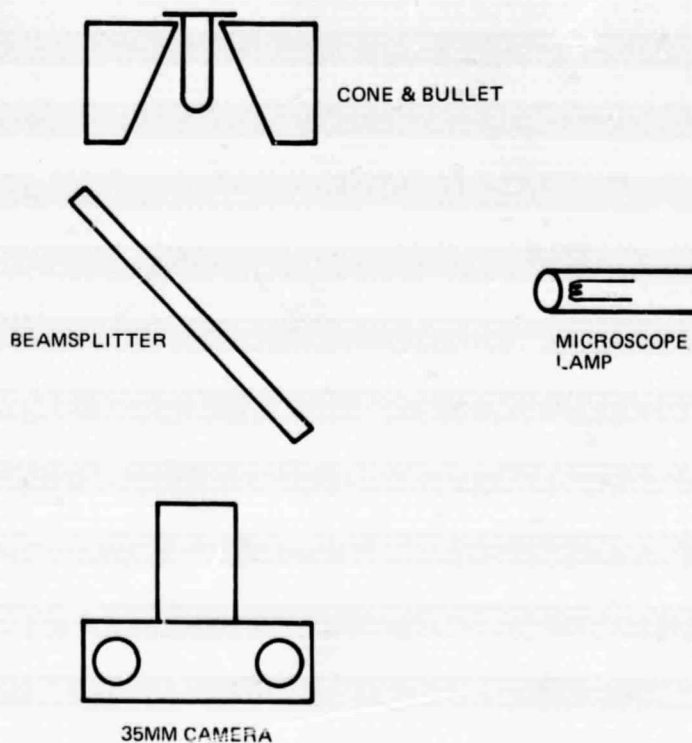


**Fig. 6 Lamp & Beamsplitter Technique for Cone Illumination**



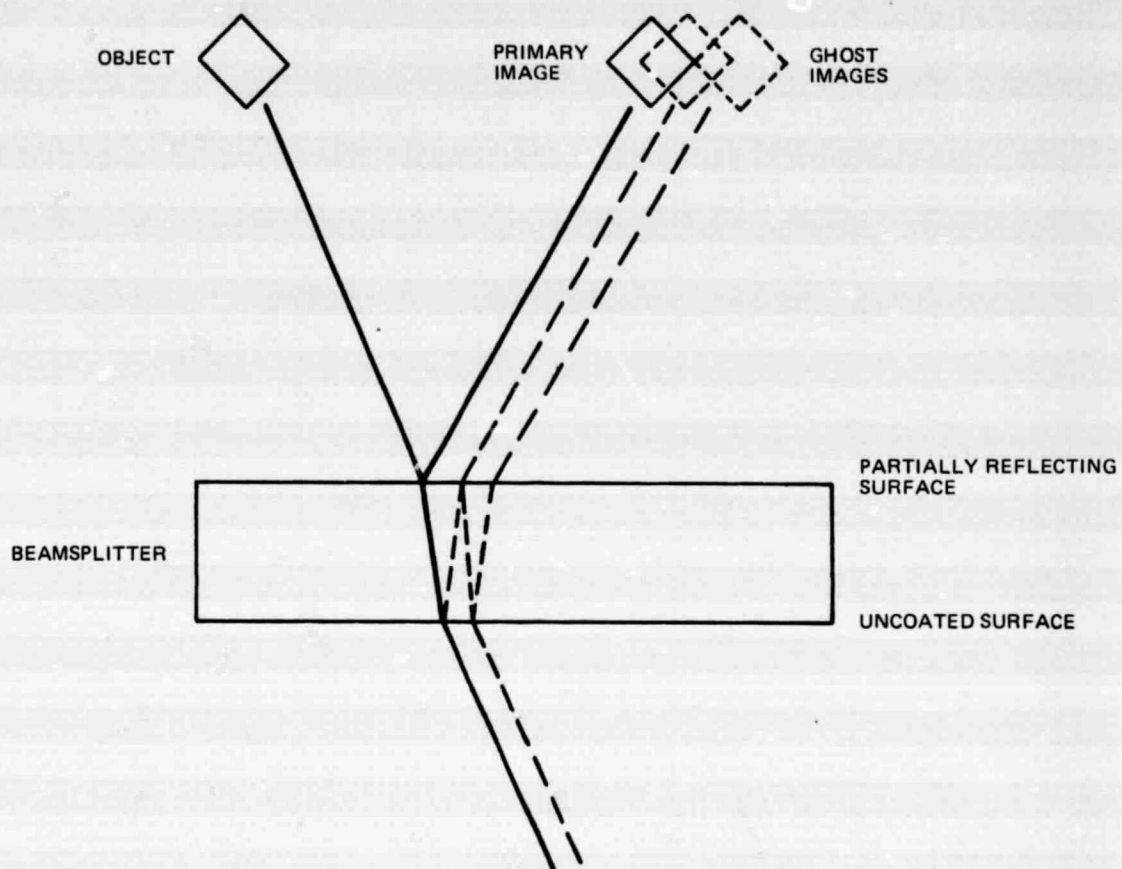


**Fig. 7 Ghost Images Formed by Beamsplitter**



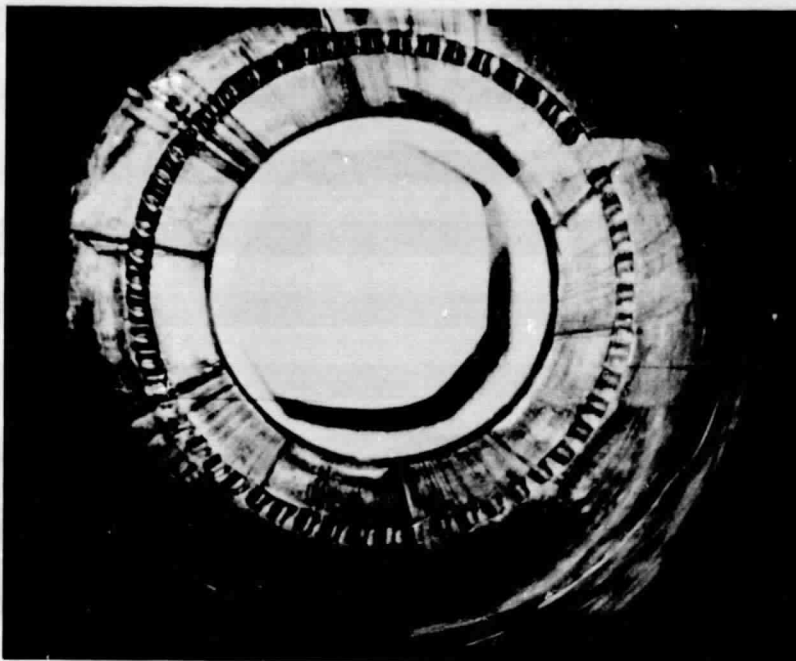


**Fig. 8 Ghost Image Formed to the Right of D.C. Stop**

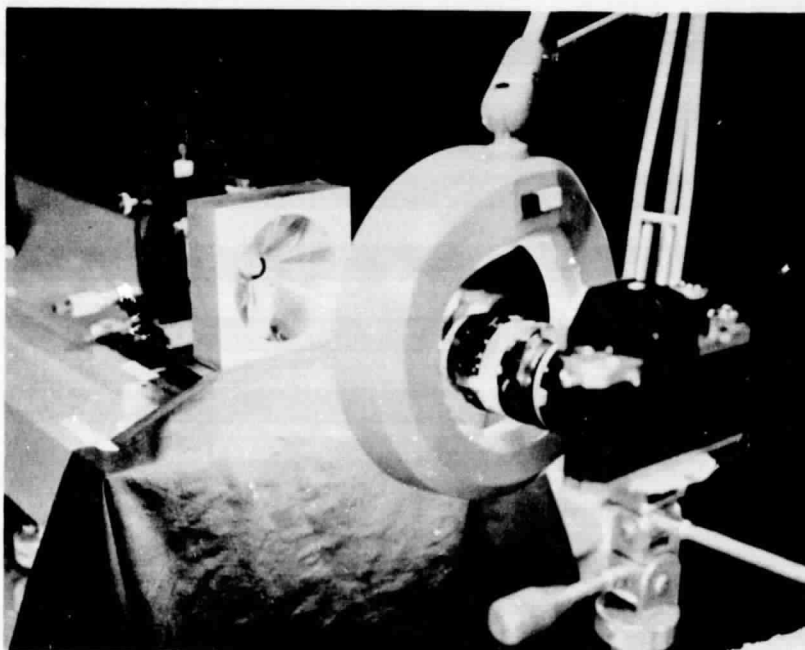


**Fig. 9 Setup Used to Photograph Bullets for Unitech, Inc. & GAC**

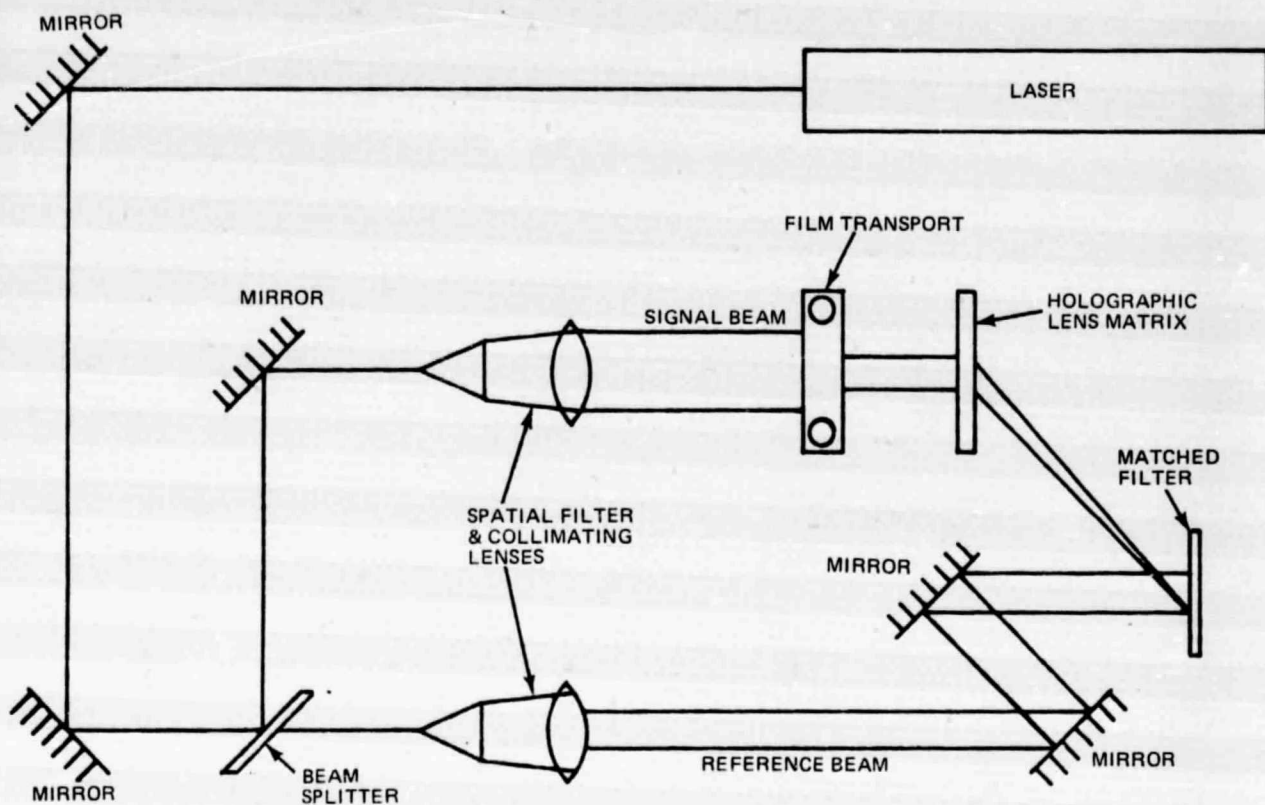
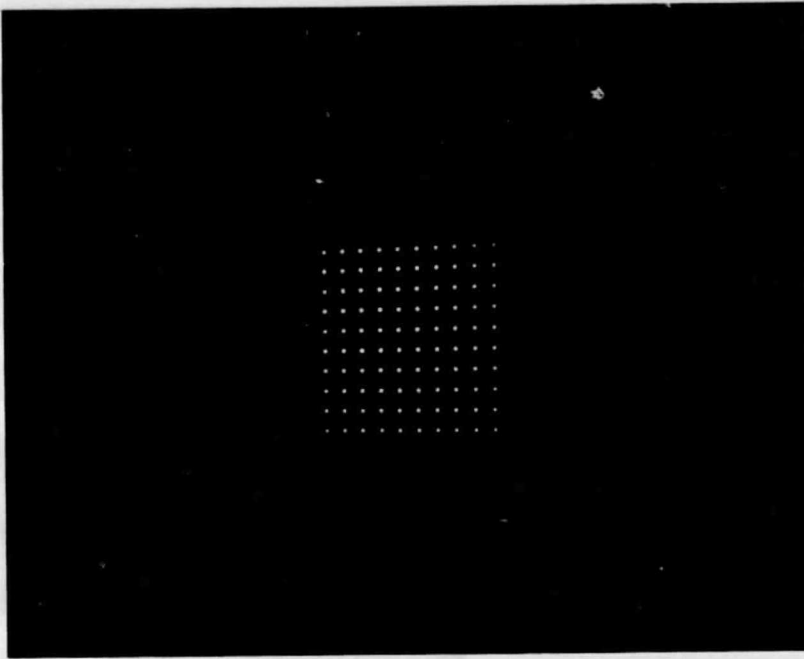
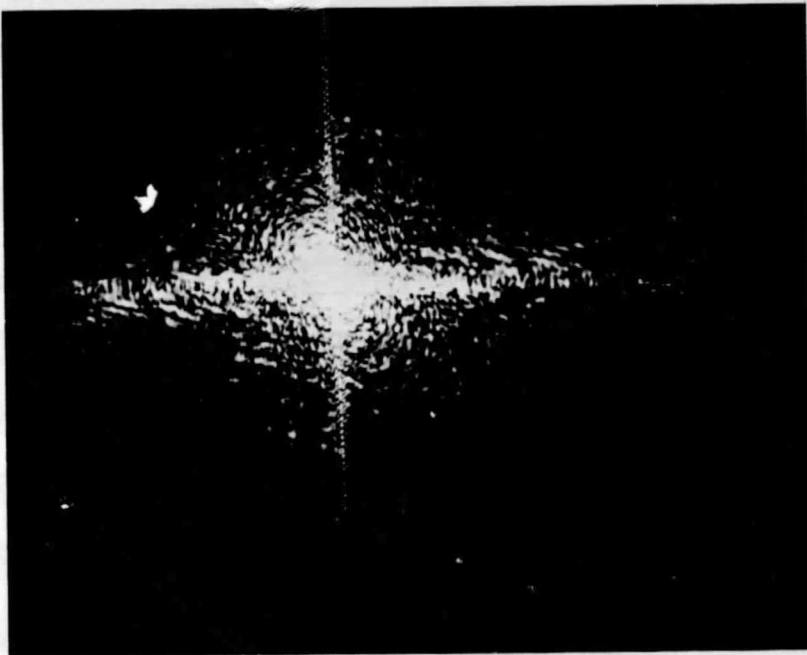


Fig. 10 Schematic Drawing of GAC Optical Signal Processor



**Fig. 11 Holographic Lens 10 x 10 Matrix**



**Fig. 12 Diffraction Pattern of Bullet B-10**

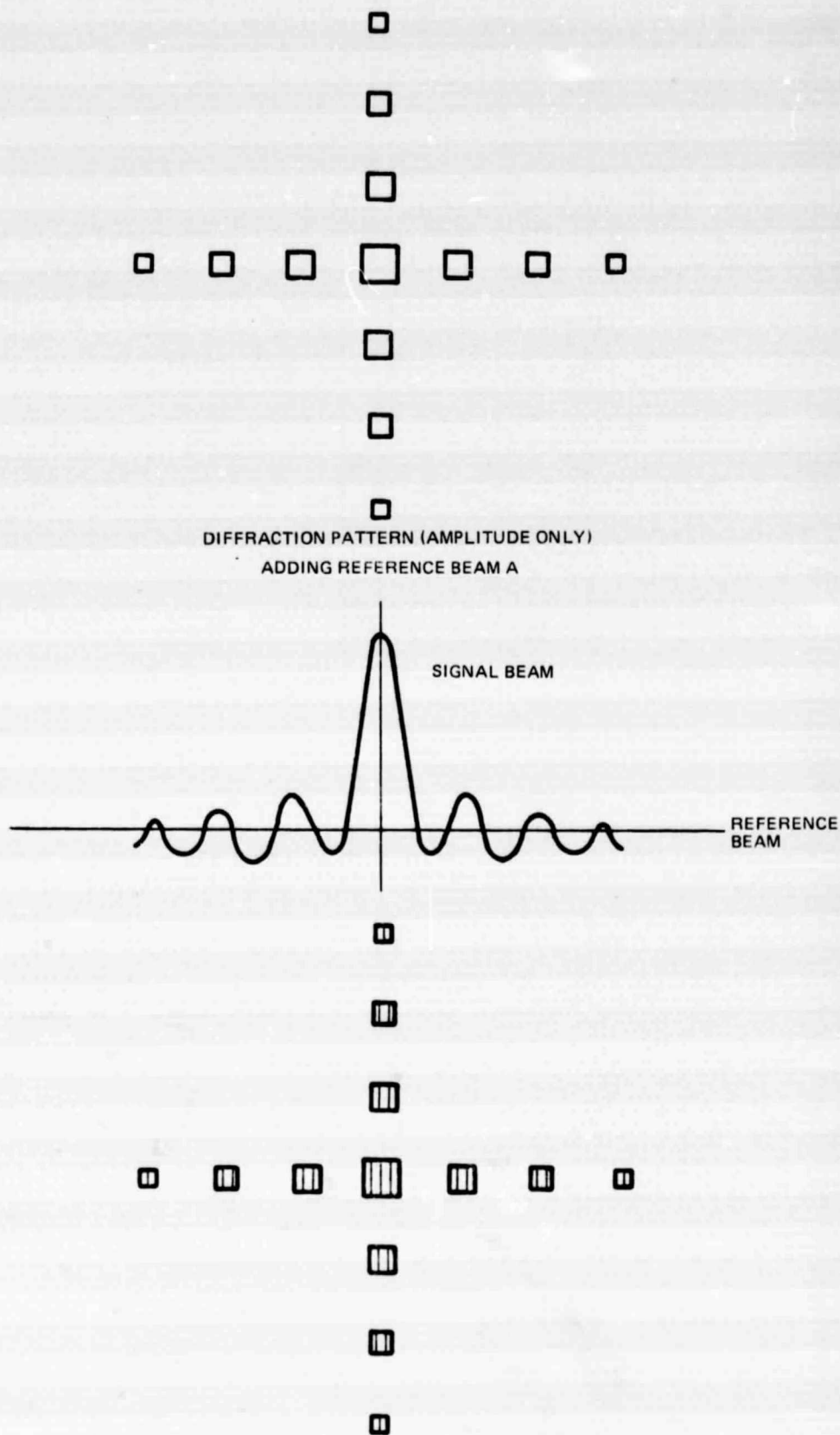


Fig. 13 Amplitude & Phase Lines Recorded as a Matched Filter



**Fig. 14 Magnified View of Match Filter. Note Grating Lines Which are Indicative of Bandpass Location**

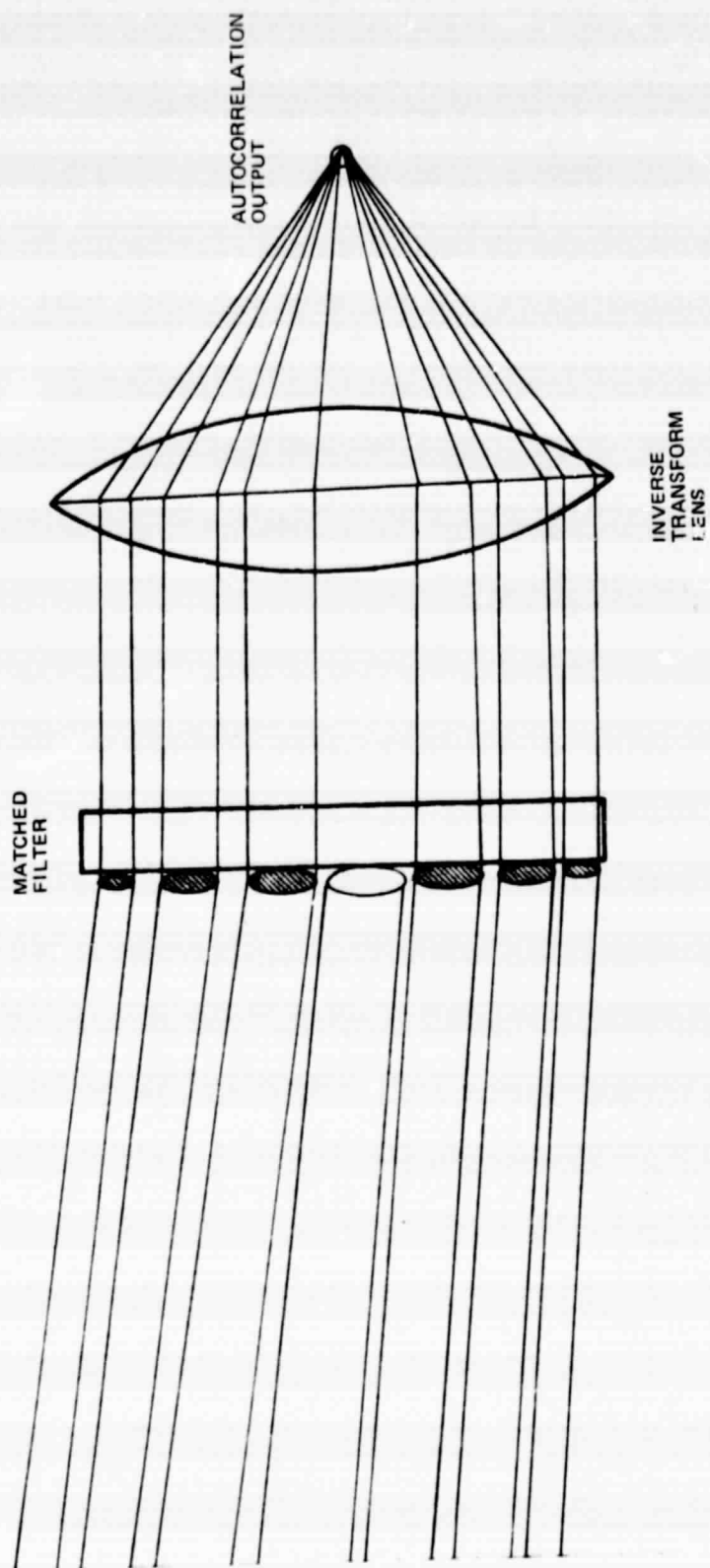
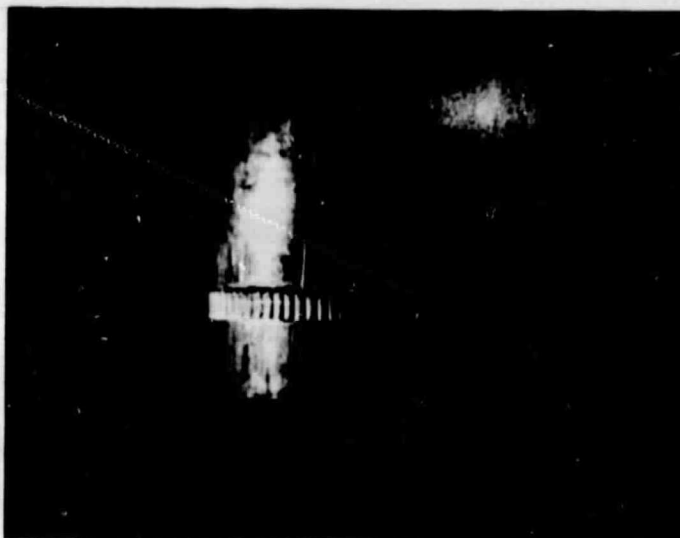
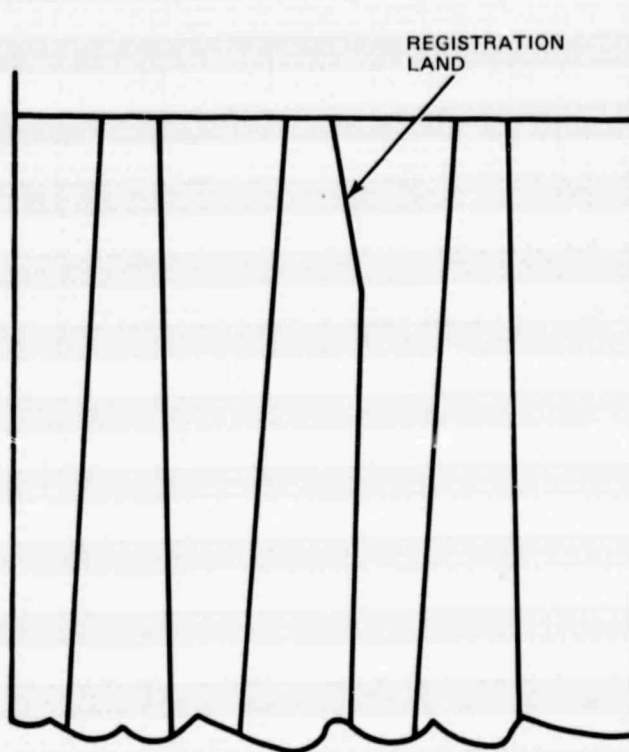


Fig. 15 Generation of Autocorrelation Signal by Matched Filter



**Fig. 16 Photograph of Side View of Bullet**



**Fig. 17 Side View of Bullet Showing Land Used for Registration**



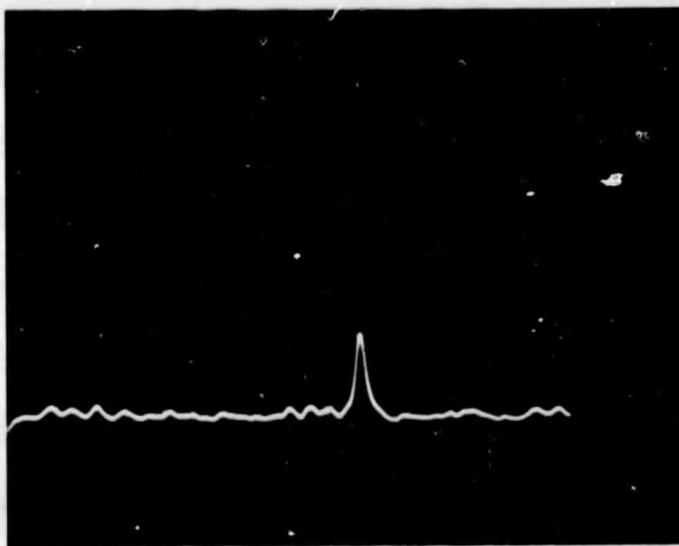


Fig. 18 Oscilloscope trace of A-5 Output.

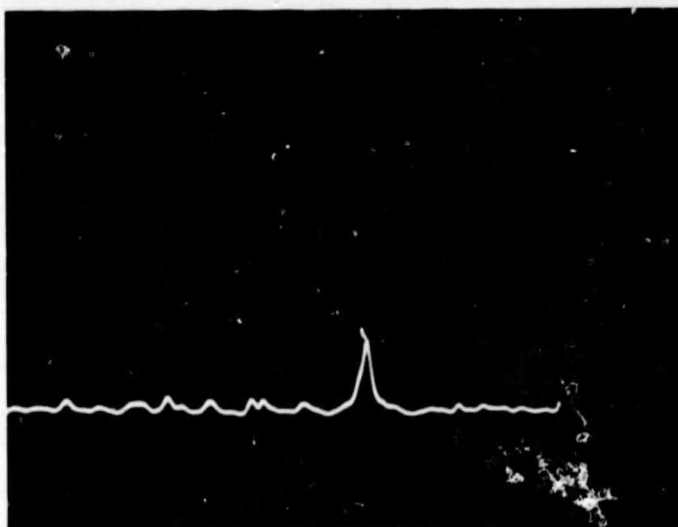
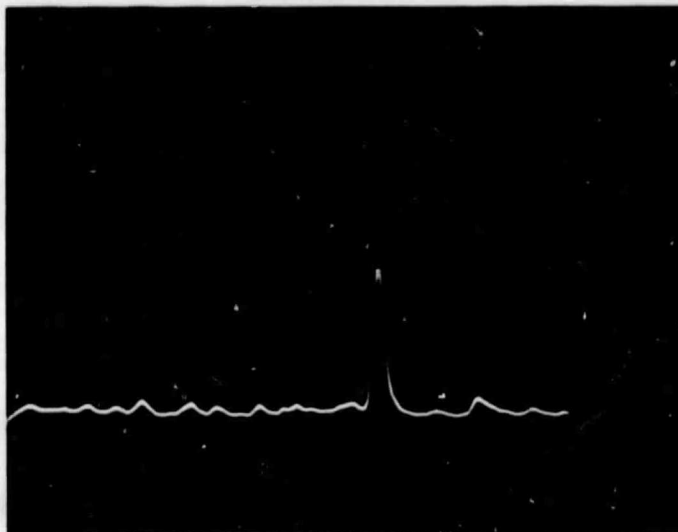
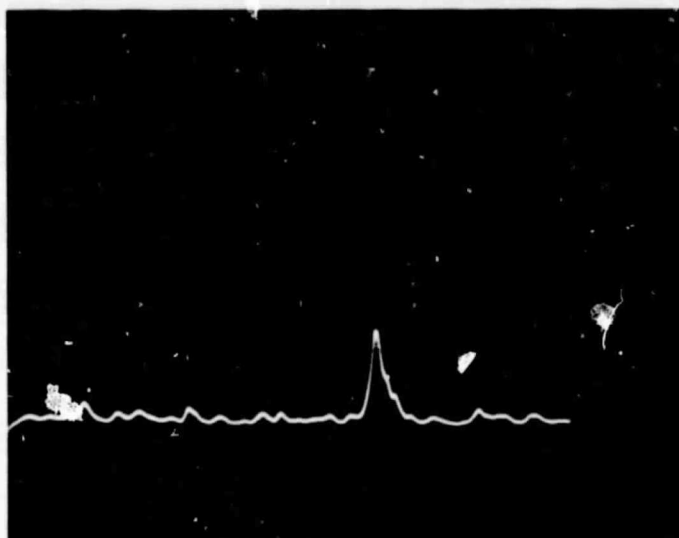


Fig. 19 Oscilloscope trace of A-6 Output.



**Fig. 20 Oscilloscope Trace of A-7 Output.**



**Fig. 21 Oscilloscope Trace of A-8 Output.**

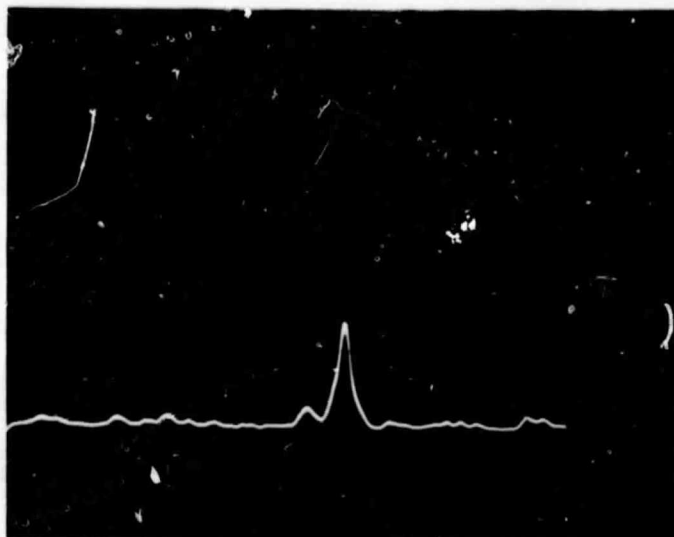


**Fig. 22 Oscilloscope Trace of B-7 Output.**

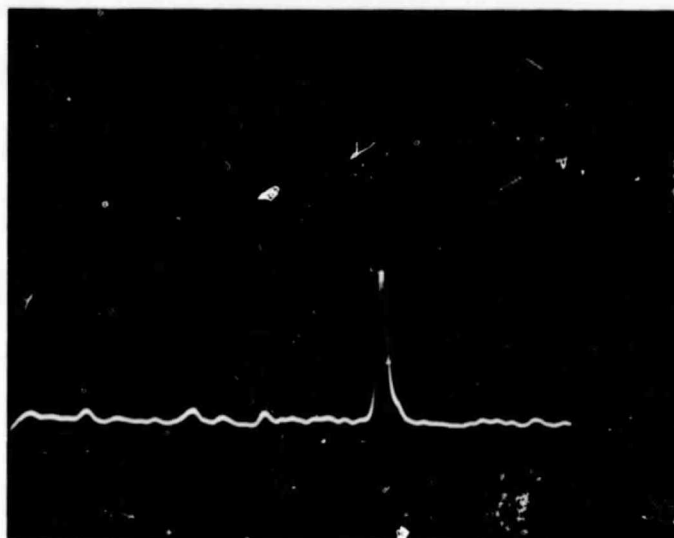


**Fig. 23 Oscilloscope Trace of B-8 Output.**

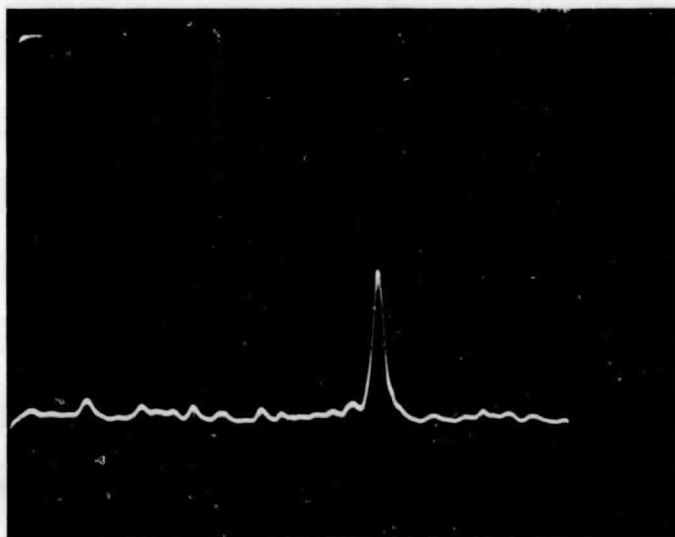


Fig. 24 Oscilloscope Trace of B-9 Output.

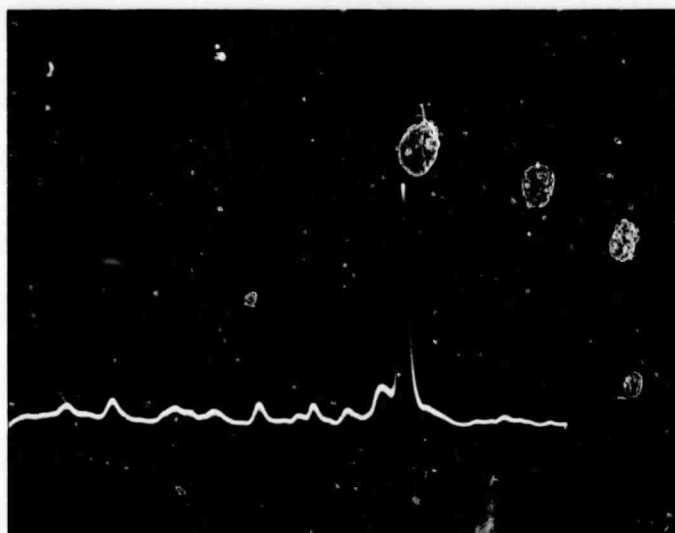
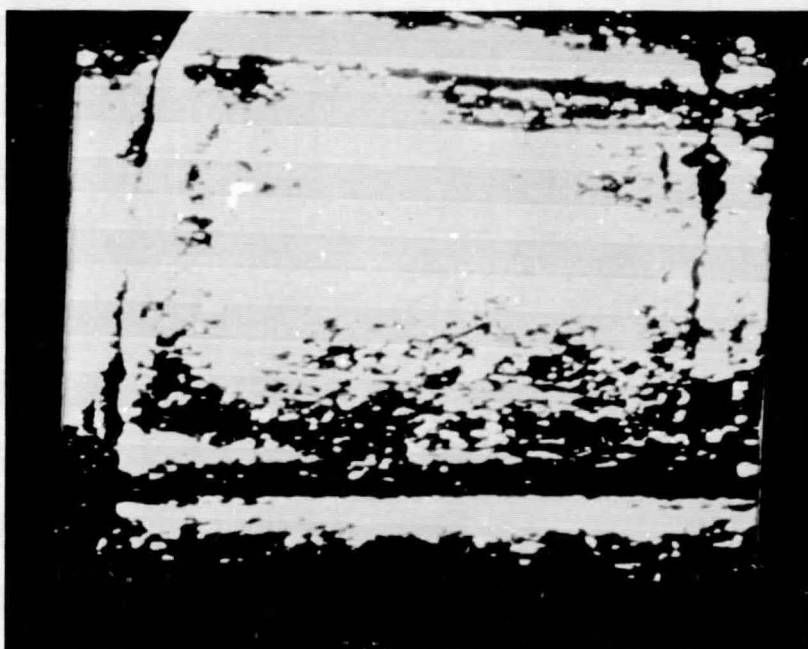


Fig. 25 Oscilloscope Trace of B-10 Output.



**Fig. 26 Magnified View of B Bullet Surface.**



**Fig. 27 Magnified View of Another B Bullet Surface.**

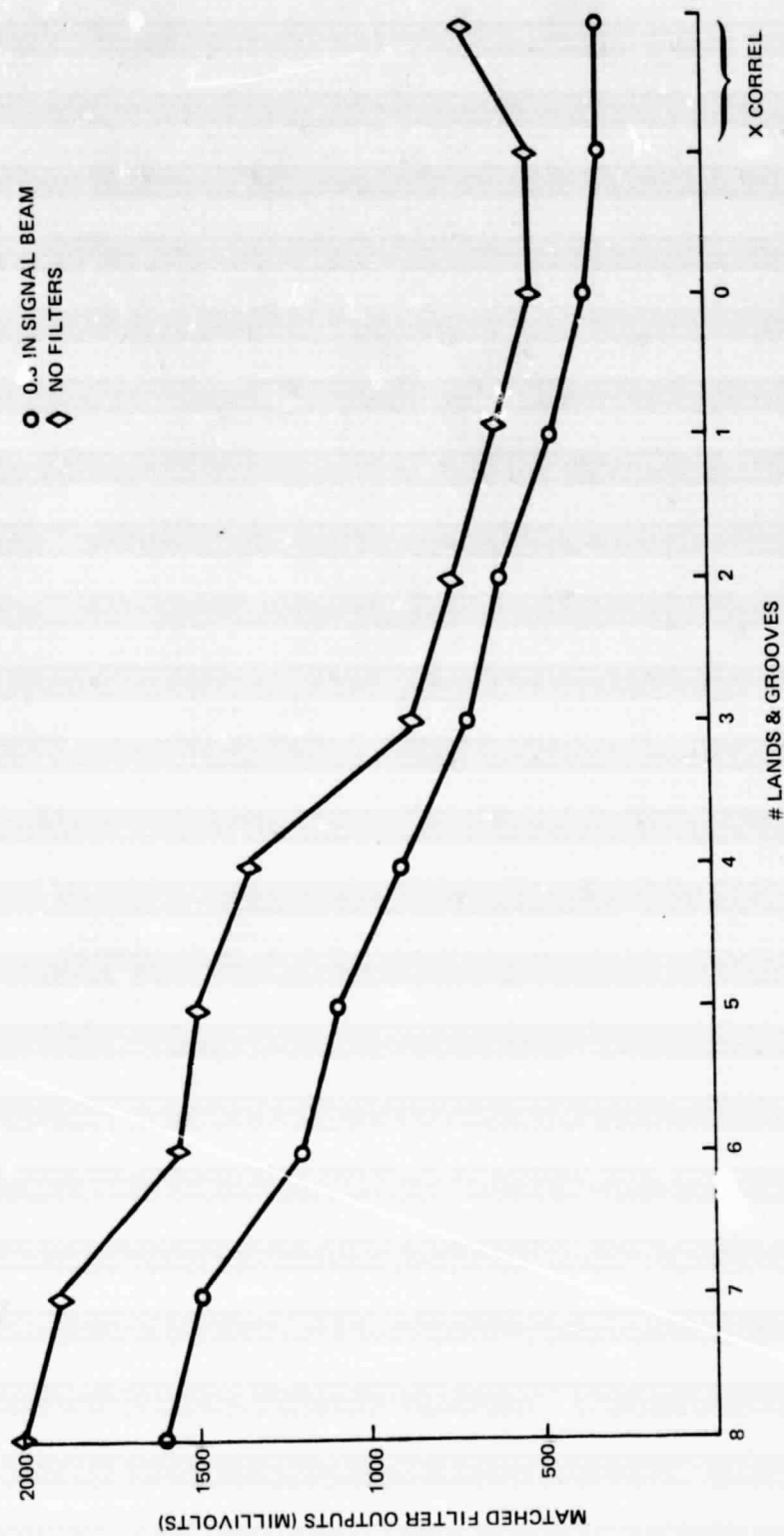


Fig. 28 Model Bullet Autocorrelation Signals (Varying Beam Ratios)

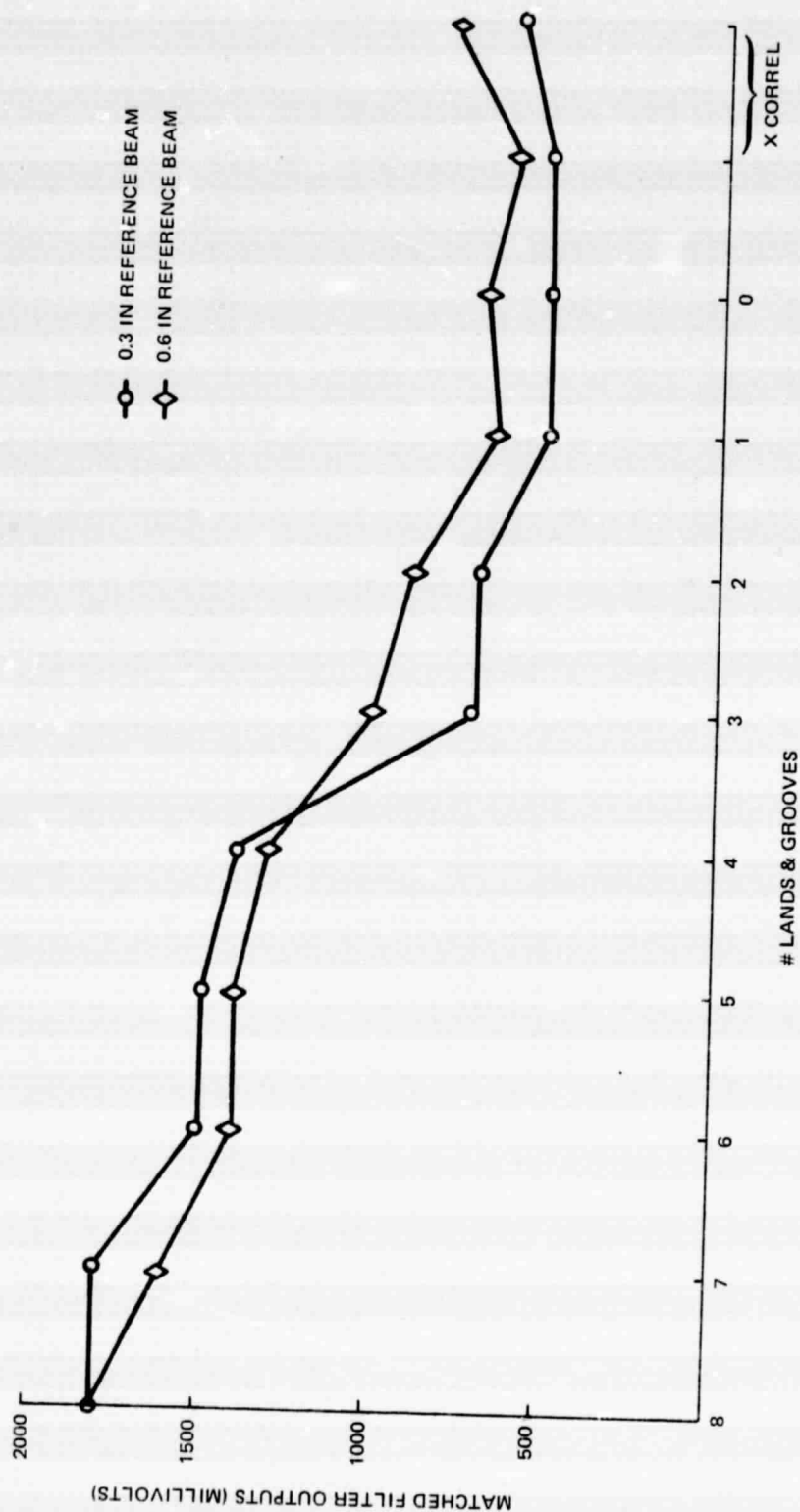


Fig. 29 Model Bullet Autocorrelation Signals (Varying Beam Ratios)



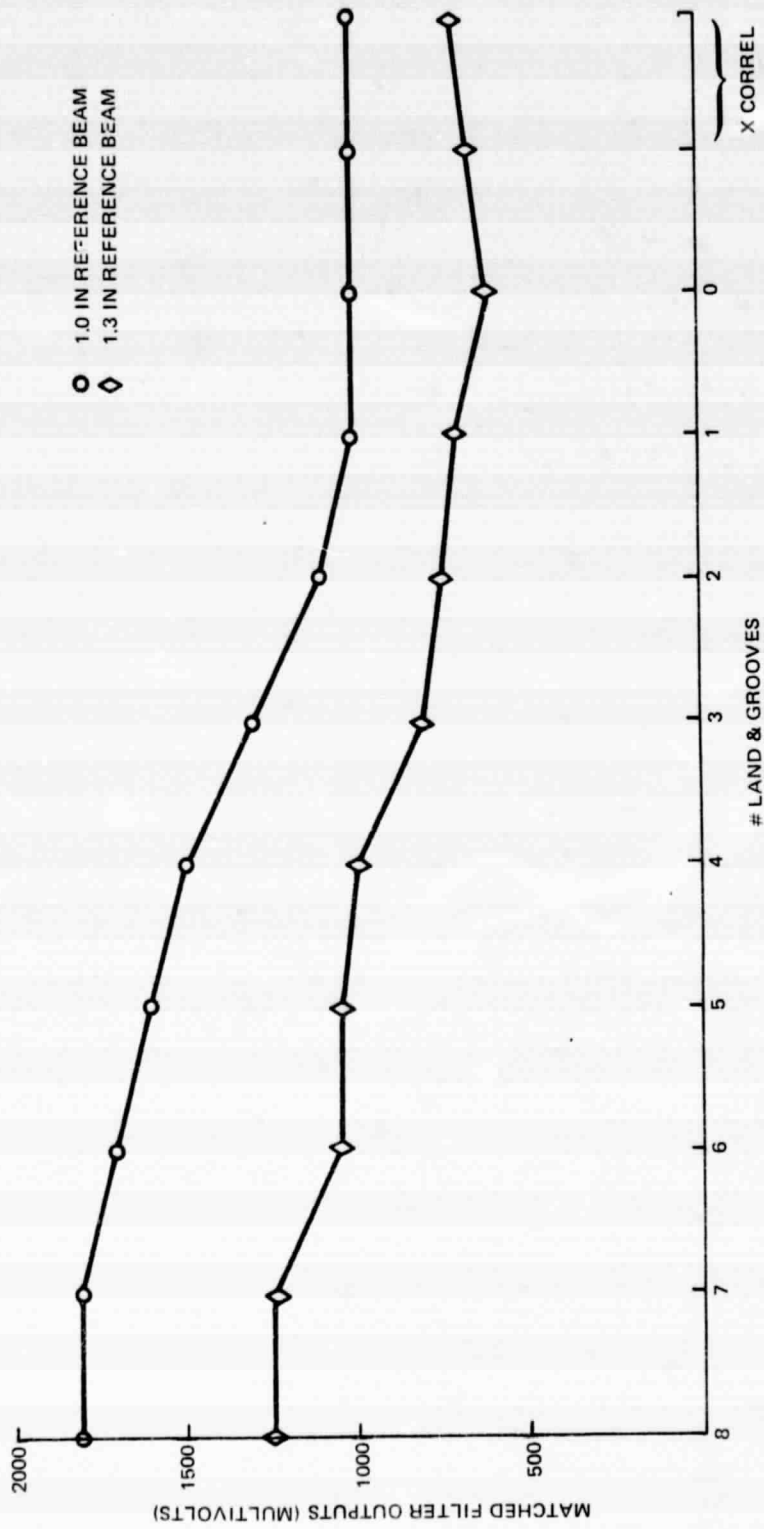
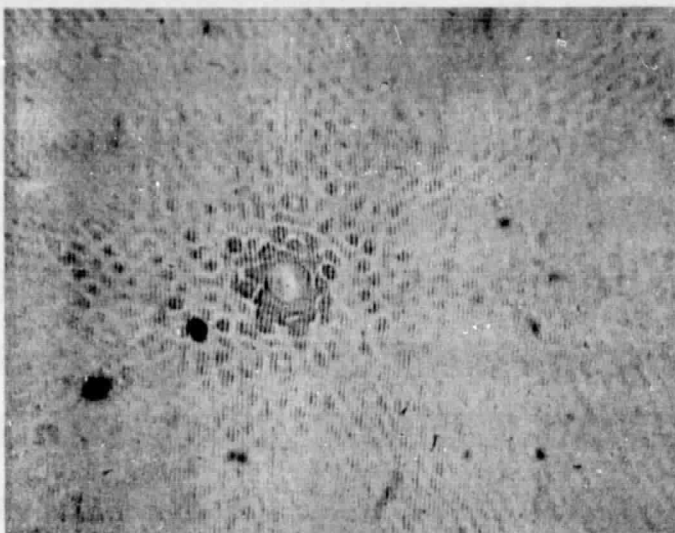
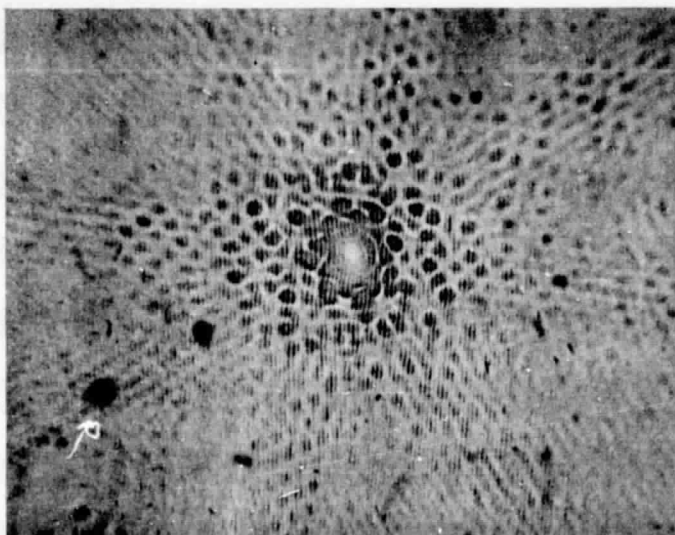


Fig. 30 Model Bullet Autocorrelation Signals (Varying Beam Ratios)



**Fig. 31 Matched Filter With 0.3 Neutral Density Filter in the Signal Beam.**



**Fig. 32 Matched Filter With no Neutral Density Filters in the Signal Beam.**

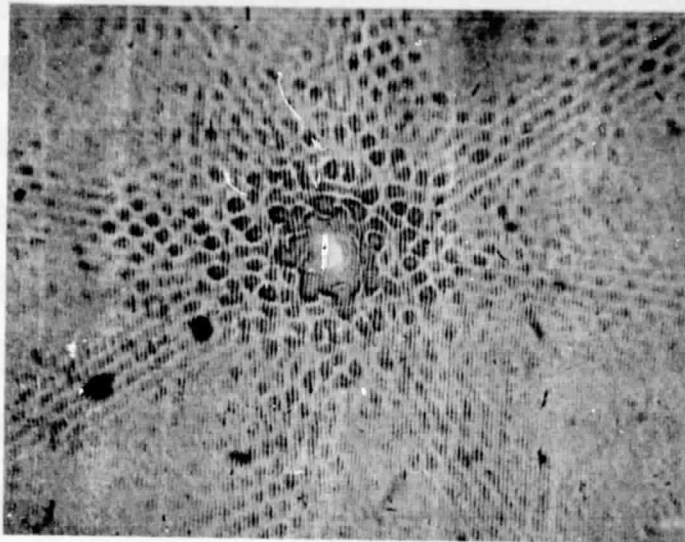


**Fig. 33 Matched Filter Using a 0.3 Neutral Density Filter in the Reference Beam.**

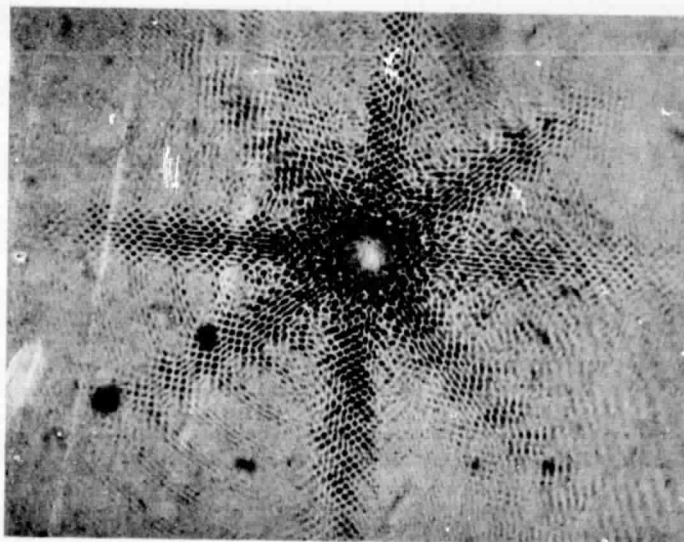


**Fig. 34 Matched Filter Using a 0.6 Neutral Density Filter in the Reference Beam.**

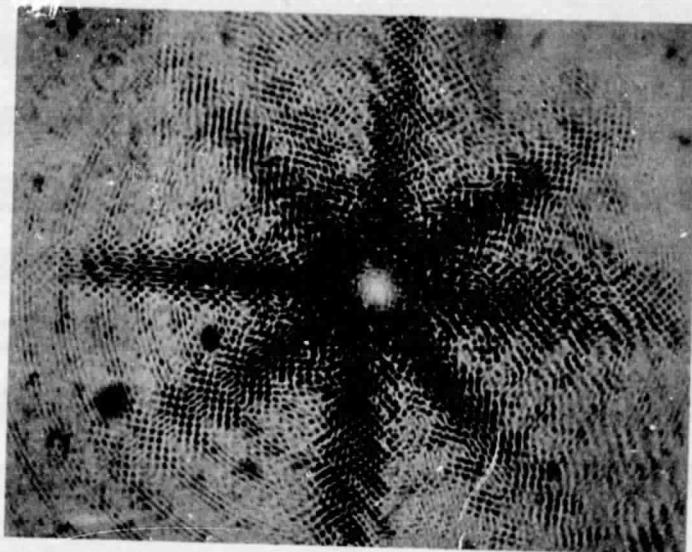


**Fig. 35 Matched Filter Using 1.0 Neutral Density Filter in the Reference Beam.**

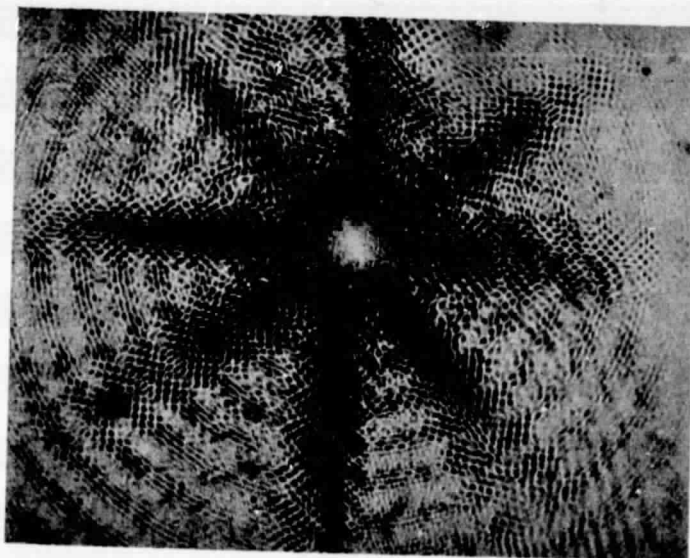


**Fig. 36 Matched Filter Using 1.3 Neutral Density Filter in the Reference Beam.**



**Fig. 37 Magnified View of Photopolymer Recording of a Bullet Surface.**

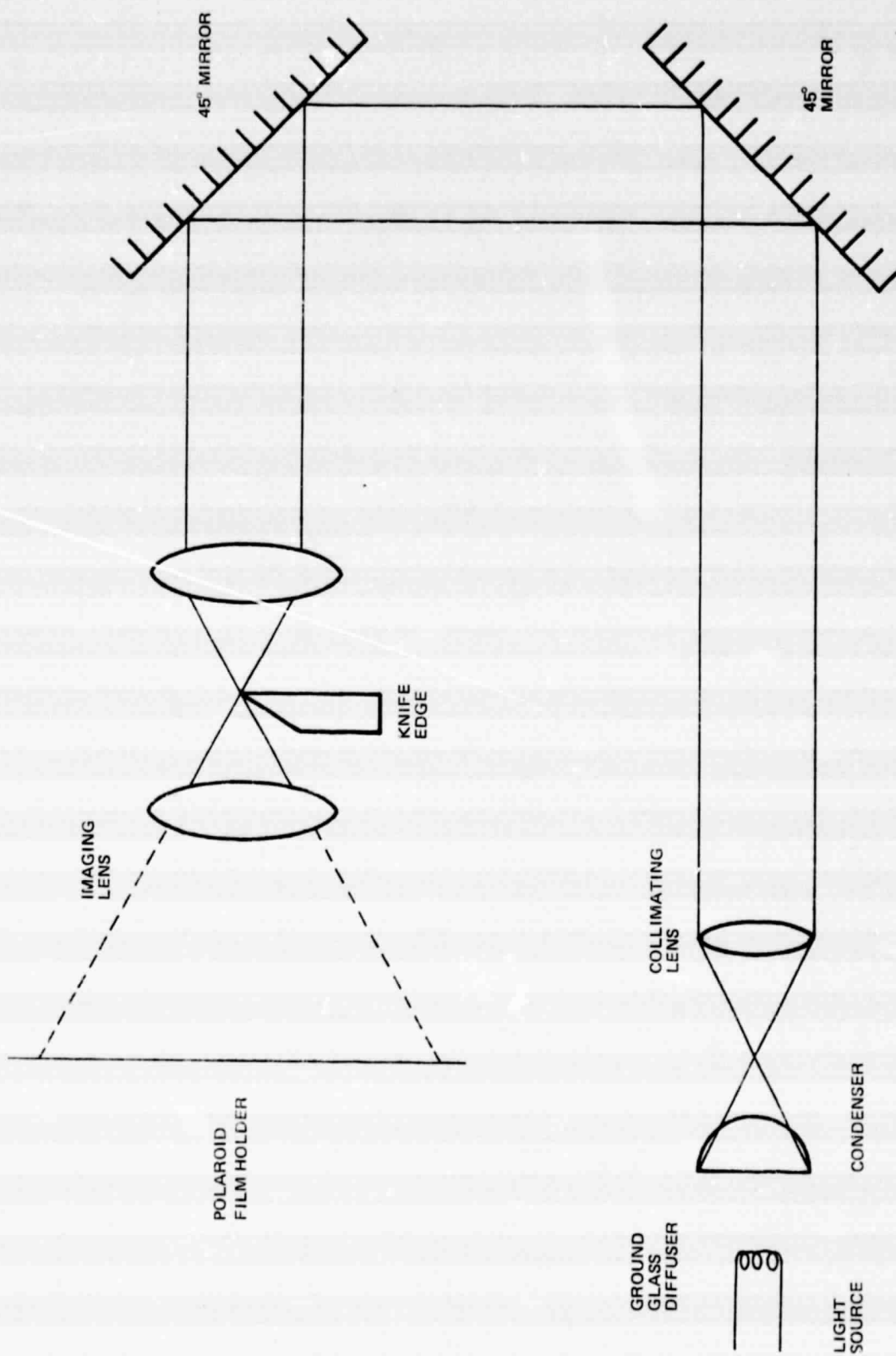


Fig. 38 Schlieren Schematic



## Appendix A

# SCHLIEREN PHOTOGRAPHY

Schlieren photography, a procedure unknown to most technologists a few years ago, is fast becoming a nearly indispensable tool for investigating the flow of gases. Particularly is this true in aeronautical engineering, where a knowledge of the flow patterns of air over surfaces becomes increasingly important as aircraft speeds approach and surpass the speed of sound. In the study of ballistics, schlieren photography discloses valuable information about shock waves accompanying projectiles. The combustion engineer uses the schlieren method in studying how fuels burn, and investigations of heat transfer are aided by the ability of schlieren photography to show the paths taken by air passing over a hot surface. In general, the schlieren technique can be used to advantage whenever it is desirable to visualize the flow of gases.

Being optical, schlieren methods do not interfere with the subject being observed. Normal motion of gases is not impeded, as is the case when pitot tubes or yaw heads are inserted in the gas stream to detect flow direction. This is particularly valuable at high gas velocities, where shock waves set up by probes in the stream may seriously distort the data.

The sensitivity of the schlieren method can be made surprisingly great. It can easily detect temperature differences as small as 10 degrees Fahrenheit in an air stream. This is adequate to disclose the currents of heated air rising from a person's fingers. Conversely, the sensitivity can be reduced to the point where the exhaust of a liquid-fueled rocket with a total temperature of more than 5,000 degrees Fahrenheit can be recorded to show the presence of shock waves and other flow phenomena.

Other optical methods also are commonly used for visualizing gas flow. Most important of these are the *interferometer* method and *shadow* photography. Neither is so widely used for visualizing gas flow as is the schlieren method. The interferometer has the characteristic of producing an image in which the differences in density are proportional to the differences in refractive index in the field. Thus, it is adaptable to quantitative measurements. With shadow photography, the differences in density of the image are proportional to the derivative of the gradient in refractive index. It is most useful in cases where the gradients are numerous and changing rapidly. Schlieren photography, intermediate between these two extremes, indicates the gradient in refractive index. Its capabilities are adequate for the majority of cases where flow patterns are of interest. Combinations of the three methods sometimes are used.

A major disadvantage of the interferometer for investigating gas flow is its great cost to assemble. Also, much care must be taken in adjusting the instrument, and the results are usually difficult to interpret. Shadow photographs, on the other hand, are easily taken with a minimum of equipment, but the results are not very useful unless the subject has strong gradients in the index of refraction.

The schlieren method offers a good compromise. The equipment needed is relatively simple and inexpensive, it can be used under widely varying experimental conditions, the sensitivity of the system can be varied at will to suit test requirements, the results are not difficult to interpret, and quantitative measurements can be obtained under idealized test conditions.

## GENERAL PRINCIPLE OF THE SCHLIEREN METHOD

Based on an optical principle generally credited to Toepler<sup>(1)</sup> and amplified extensively by Schardin,<sup>(2)</sup> the schlieren method depends upon refraction of the narrowly defined edge of a light beam by gradients in the refractive index of the gas through which the beam of light passes. Thus, it receives its name "schlieren," which is translated as "optical inhomogeneity." In a typical system, a limiting diaphragm, usually a straightedge, is so adjusted with respect to the edge of the light beam that refraction in one direction adds to the total illumination, and refraction in the other direction subtracts from it. Thus, an image is formed wherein the variations in brightness depend upon differences in the gradients of refractive index in the light path.

Figure 1 shows the simplest type of schlieren system. Light from the source, which is preferably a line rather than a point, is focused by the condenser to form an image. A limiting diaphragm, generally straight rather than circular, is placed parallel to this image of the light source and intercepts part of it so that the resultant beam has a sharply defined edge. This beam then passes through the Schlieren Head, which focuses it through the Schlieren Field onto the second knife-edge. By adjusting the position of this second knife-edge so that it is exactly parallel with the first knife-edge, and by inserting it partially into the beam of light, a gate is provided that can intercept a large part of the luminous flux. This attenuated beam of light then passes to a photographic film where it can be recorded.

(1) Toepler, A. "Beobachtungen Nach Einer Neuen Optischen Methode," *Ostwalds Klassiker der exakten Wissenschaften*, No. 157, Leipzig, 1906.

(2) Schardin, H. "Das Toeplersche Schlieren-Verfahren," *Ver. Deutsch. Ing. Forschungschft*, 367, July-August, 1934.

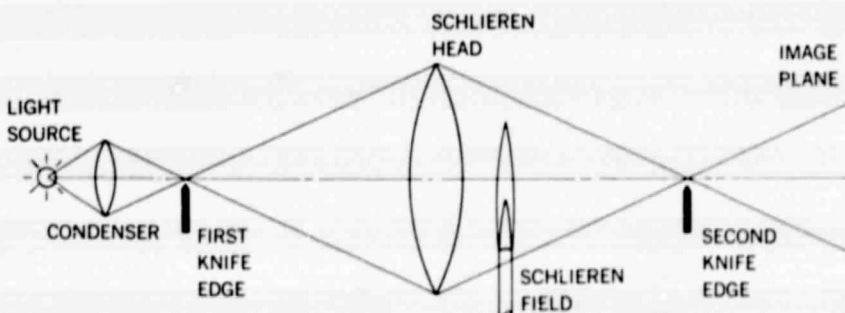


Figure 1—Basic Schlieren System

If there are no gradients in refractive index within the Schlieren Field, the amount of light reaching the film is fixed by the relative position of the two knife-edges. However, if a gradient normal to the plane of the knife-edges exists, the beam will be refracted so that it either adds to or subtracts from the light normally present on the screen. Thus, a Schlieren Field involving a pattern of gases is reproduced in various tones on the film. Opaque objects appear in silhouette.

## OPTICAL DETAILS OF SCHLIEREN EQUIPMENT

Most literature on the schlieren method describes only specific systems or its use for a given problem. Liepmann and Puckett<sup>(3)</sup> and Lewis and von Elbe<sup>(4)</sup> review schlieren systems in general and point out their application for general scientific purposes. Barnes and Bellinger<sup>(5)</sup> summarize schlieren methods in considerable detail and provide an extensive bibliography on the subject.

Optical equipment not commonly available commercially is needed in designing schlieren systems. Therefore, technologists usually design and construct schlieren apparatus for their own particular needs. The following design considerations will be helpful in deciding on components for specific applications.

### Formation of the Schlieren Image

Formation of the schlieren image depends essentially upon two superimposed optical systems. One provides general illumination of the field and forms a silhouette image of opaque subjects. The other produces variations in light intensity within the subject area for transparent subjects, depending upon how the light is refracted by gradients in the index of refraction in the Schlieren Field.

Figure 2 illustrates how this double image is produced. The Schlieren-Head lens  $H$  forms an image of the light source  $S$  at  $S'$ , passing through the Schlieren Field  $F$ . The objective lens  $O$  then illuminates the screen  $I$ . At the same time, the objective lens  $O$  forms a real image of the point  $A$  at  $A'$ , the planes  $F$  and  $I$  being conjugate about  $O$ . Most important is the fact that all rays of light passing through any point in plane  $F$  will form a real image at  $I$ , irrespective of the angle at which the rays pass through plane  $F$ . Thus, any object in the Schlieren Field, plane  $F$ , will produce a real image at plane  $I$ .

Because the presence of a gradient in refractive index at plane  $F$  will cause the rays of light to be refracted, say upward as at  $A$ , the image which they form at  $S''$  will be displaced from the normal position at  $S'$ . This displacement  $d$  will depend upon the angle  $\alpha$ , known as the "angular deviation," through which the rays were bent. Thus, all rays passing through  $A$  intersect the image plane  $I$  at  $A'$  to form a real image, and  $A$  also receives light from all points of the source  $S$  so that light passing through  $A$  produces an image of the source.

[3] Liepmann, H. W., and Puckett, A. E. *Introduction to Aerodynamics of a Compressible Fluid*. John Wiley and Sons, Inc., New York, 1947, pp 89-101.

[4] Lewis, B., and von Elbe, G. *Combustion, Flames and Explosions of Gases*. Academic Press Inc., New York, 1951, pp 211-218.

[5] Barnes, N. F., and Bellinger, S. L. "Schlieren and Shadowgraph Equipment for Air Flow Analysis," *J. Opt. Soc. Amer.*, Vol. 35, No. 8, pp 497-509.

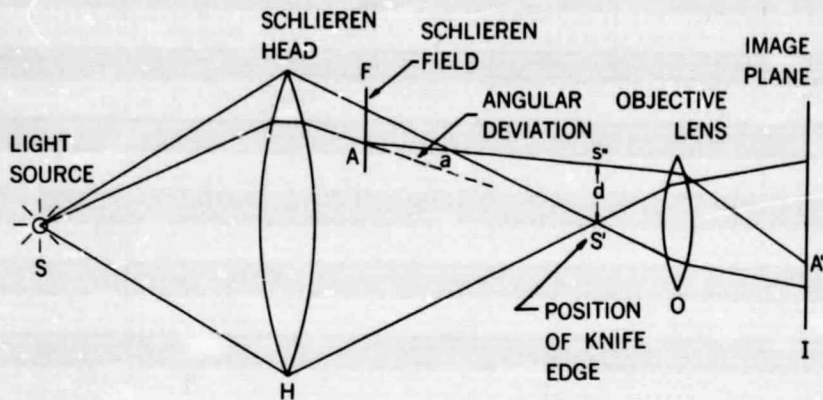


Figure 2—Formation of Schlieren Image

The two independent modes of formation of the schlieren image, therefore, are: (1) displacement of the image of the source by the angular deviation produced by a refractive-index gradient in the Schlieren Field, and (2) formation of a real image of the Schlieren Field at the film plane. For the first case, the displacement is unaffected by the position of the point in the Schlieren Field; and for the second, the image formed is independent of the angular deviation.

The average intensity of illumination of the image field is fixed by the position of the second knife-edge normal to the bundle of light rays at  $S'$ . Usually, the knife-edge is adjusted so that the brightness is about midway between full illumination and complete extinction. Varying the position of this knife-edge also affects the sensitivity of the system. Generally, as sensitivity is easily judged visually, no critical adjustments are involved. However, in extremely high-speed applications, a micrometer-type adjustment mechanism for the knife-edge should be used.

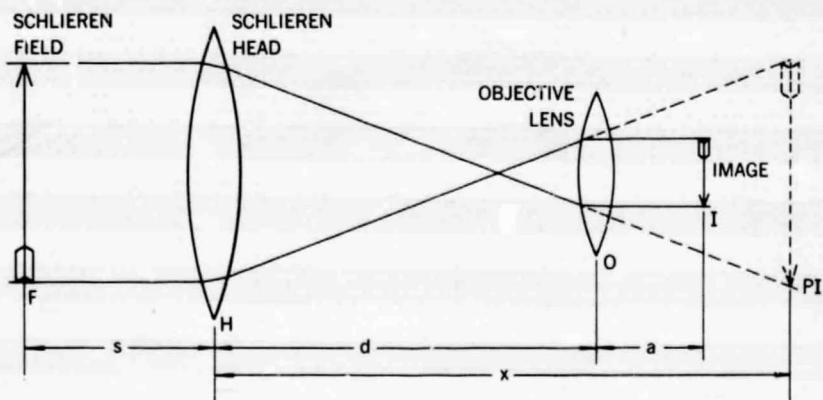


Figure 3—Location of Schlieren Image Plane

### Location of Image Plane

Simple optical relationships fix the location of the image plane.<sup>(6)</sup> For simplicity, assume a two-element schlieren system where a parallel beam of light passes through the Schlieren Field.

Figure 3 shows the optical paths. If the objective lens were not present, the Schlieren Head  $H$  would form a primary image  $PI$  of the field  $F$ . From the thin lens formula, the distance  $x$  of this image would be equal to the Field distance  $s$  times the focal length of the Head  $F_H$ , divided by their difference—

$$x = \frac{s \cdot F_H}{s - F_H} \quad (1)$$

When the objective or camera lens is added to the system, this primary image becomes its subject which, in turn, is imaged on the film. The lens-to-film distance or camera extension  $a$  can be found by

$$a = \frac{F_o \cdot (d - x)}{d - x - F_o} \quad (2)$$

where  $d$  is the separation between the Schlieren Head and the objective lens.

It should be noted that the position of the primary image  $PI$ , and thus the sign of  $x$ , will depend on the relation between  $s$  and  $F_H$ . When  $s$  is greater than  $F_H$ ,  $PI$  is a real image formed somewhere to the right of  $H$ , and  $x$  is positive. When  $s$  is less than  $F_H$ ,  $PI$  is a virtual image to the left of  $H$ , and  $x$  is negative.

(6) Keagy, W. R., Ellis, H. H., and Reid, W. T. *Schlieren Techniques for the Quantitative Study of Gas Mixing*. Report R-164, The RAND Corporation, Santa Monica, Calif., 1949, 57 pp.

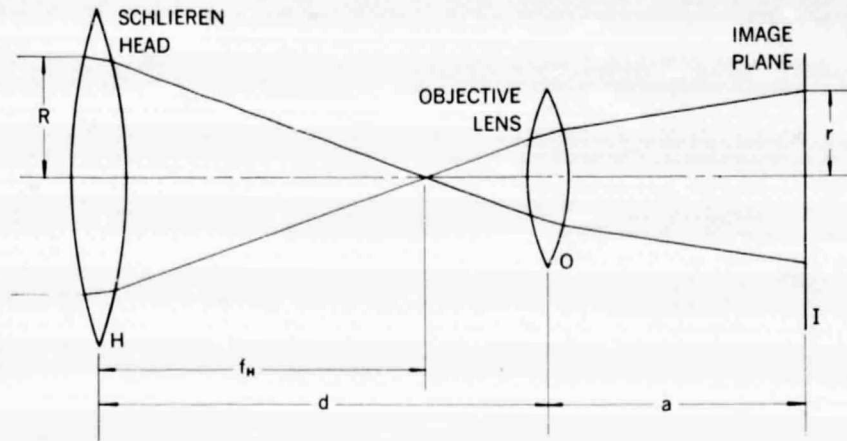


Figure 4—Size of Image Field in Schlieren System



### Size of the Image Field

The magnification of the image, or the ratio between the size of the image and the size of the field, is equal to the magnification between the field and primary image ( $m_H$ ) multiplied by the magnification between the primary image and the camera image ( $m_o$ ), Figure 4. These can be found from the following relations:

$$m_H = \frac{F_H}{s - F_H} \text{ and} \quad (3)$$

$$m_o = \frac{F_o}{F_o + x - d} \quad (4)$$

Since  $x$  cannot be measured directly, it is more convenient to substitute its value in terms of  $s$  and  $F_H$  from equation (1). With this substitution, and multiplying (3) by (4),

$$\text{Magnification} = \frac{r}{R} = \frac{F_H \cdot F_o}{s \cdot (F_o + F_H) + d \cdot (F_H - s) - F_o \cdot F_H} \quad (5)$$

As an example, assume:

Focal length of Schlieren Head =  $F_H = 100$  inches,

Focal length of Objective Lens =  $F_o = 10$  inches,

Distance from Schlieren Head to Field =  $s = 200$  inches, and

Distance between Schlieren Head and Objective Lens =  $d = 120$  inches.

Calculate the position of the image plane and the relative size of the image compared with the field:

### The position of the primary image

$$x = \frac{s \cdot F_H}{s - F_H} = \frac{200 \cdot 100}{200 - 100} = 200 \text{ inches}$$

### Objective lens-to-film distance

$$\begin{aligned} a &= \frac{F_o \cdot (d - x)}{d - x - F_o} = \frac{10 \cdot (120 - 200)}{120 - 200 - 10} \\ &= \frac{-800}{-90} = 8.9 \text{ inches} \end{aligned}$$

### Magnification, ratio of image to field,

$$\begin{aligned} \frac{r}{R} &= \frac{F_H \cdot F_o}{s(F_H + F_o) + d(F_H - s) - F_o \cdot F_H} \\ &= \frac{100 \cdot 10}{200 \cdot (100 + 10) + 120 \cdot (100 - 200) - 100 \cdot 10} \\ &= \frac{100 \cdot 10}{200 \cdot 100 - 120 \cdot 100 - 100 \cdot 10} = \frac{10}{90} = 0.11 \end{aligned}$$

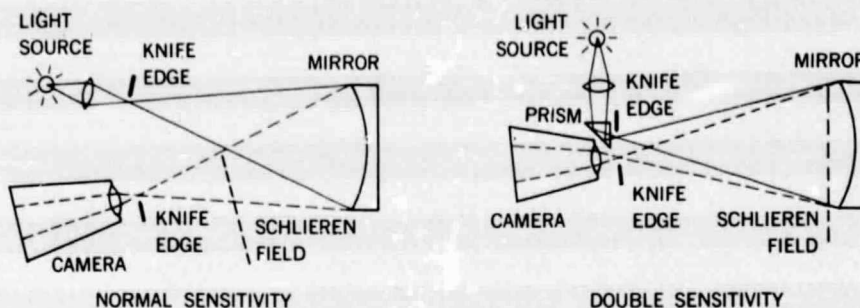


Figure 5—Typical Single-Mirror Schlieren Systems

Thus, for the stated conditions, the image will be 11 percent of the size of the object, and a field of, say, 12 inches in diameter would be recorded in a circle 1.3 inches in diameter. It should also be noted that the camera extension, or objective lens-to-film distance, of 8.9 inches is less than the focal length of the lens. Therefore, the lens board or the camera back will have to be racked in from the normal infinity position, a situation that is not encountered in conventional photography.

It is also possible to operate a schlieren system of this type without an objective lens by placing the film at the position of the primary image *PI*. In this case, only equations (1) and (3) are involved.

## ARRANGEMENT OF SCHLIEREN COMPONENTS

### Single-Element Systems

Many possible combinations of elements can be assembled to form schlieren systems. The simplest would be a system arranged according to Figure 1, with a lens of good optical quality serving as the Schlieren Head. Because lenses of adequate quality generally are not available in sizes more than a few inches in diameter, it is more convenient to use first-surface concave parabolic mirrors. Such mirrors should be figured accurately so that imperfections in the surface are not confused with the image produced by the Schlieren Field. Usually, mirrors of a grade suitable for telescopes are satisfactory. Common specifications call for mirrors figured within 0.1 wavelength of sodium light.

Figure 5 shows two typical schlieren systems using a single mirror as the Schlieren Head. That on the left is essentially the system of Figure 1, with a mirror substituted for the lens. However, because the light source and the camera cannot both be normal to the mirror, some coma is introduced by the skewness of the components. Another minor shortcoming is that the Schlieren Field must be placed well out in the converging beam from the mirror, thus limiting the size of the field as compared with the size of the mirror.

The schlieren system on the right in Figure 5 uses a prism—a first-surface mirror would do equally well—to bring the central axis of the light source nearer to that of the camera. Although coma is reduced by this expedient, its main purpose is to permit

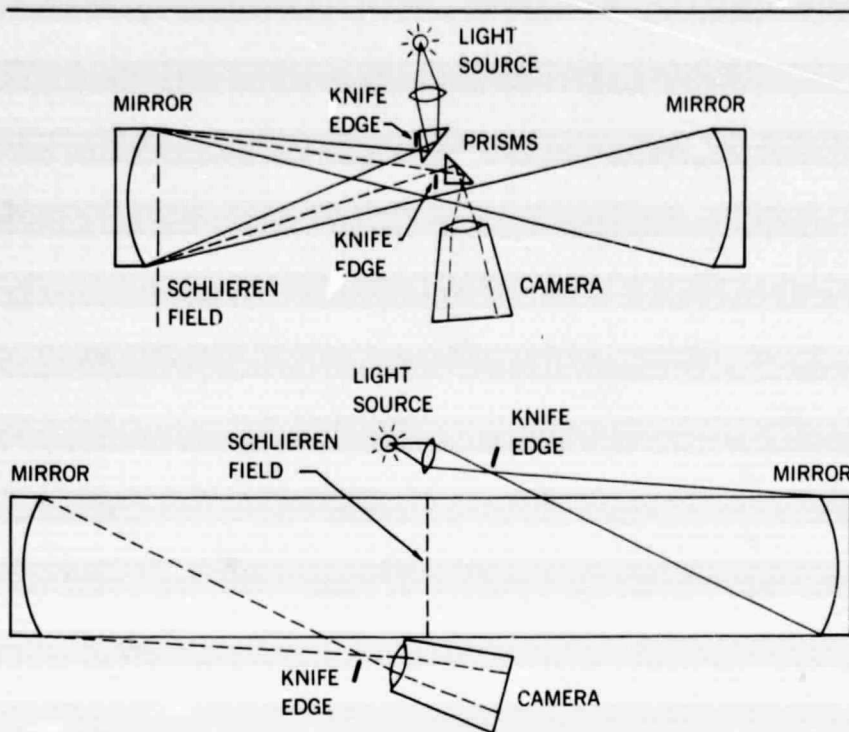


Figure 6—Two-Mirror Schlieren Systems

the light beam to pass twice through the Schlieren Field, thus doubling the sensitivity of the system over the more conventional arrangement at the left. Because the two light paths through the Field are not exactly coincident, the resolution of the image is somewhat impaired.

Many different modifications of high-sensitivity schlieren systems can be devised, with the light beam passing through the Schlieren Field as often as desired. As the number of paths becomes greater, however, the resolution of the image usually is poorer.

### Two-Element Systems

Figure 6 illustrates schlieren systems based on the use of two Schlieren Heads. Although mirrors are shown, good-quality lenses could be used.

In the upper system, the light beam passes four times through the Schlieren Field, producing high sensitivity. Except for the use of two prisms and the second Schlieren Head, this system is essentially the same as the double-sensitivity system shown in Figure 5.

The lower system of Figure 6 is the most popular of all schlieren systems. It has the unique advantage that parallel rays of light pass through the Schlieren Field, thus producing an image of superior resolution. Further, because the light source and the camera are placed on opposite sides of the light path between the mirrors, coma is cancelled. Another advantage is that the Schlieren Field is located away from the mirrors.

In fact, the least permissible separation of the mirrors is about twice their focal length in order to provide space for the Schlieren Field between the entrance and exit cones of light. On the other hand, since the light beam is parallel between the two mirrors, they can be separated as far as desired. This is particularly useful with wind tunnels where it is not convenient for the Schlieren Head to be near the Field, or with explosion or high-temperature combustion phenomena where the Schlieren Head must be protected from damage.